

1 Improving statistical power in severe 2 malaria genetic association studies 3 by augmenting phenotypic precision

4 James A Watson^{1,2†*}, Carolyne M Ndila^{1,2†}, Sophie Uyoga³, Alexander W Macharia³,
5 Gideon Nyutu³, Mohammed Shebe³, Caroline Ngetsa³, Neema Mturi³, Norbert
6 Peshu³, Benjamin Tsofa³, Kirk Rockett^{4,5}, Stije Leopold^{1,2}, Hugh Kingston^{1,2},
7 Elizabeth C George⁶, Kathryn Maitland^{3,7}, Nicholas PJ Day^{1,2}, Arjen Dondorp^{1,2},
8 Philip Bejon^{2,3}, Thomas N Williams^{3,7‡}, Chris C Holmes^{8,9‡}, Nicholas J White^{1,2‡}

*For correspondence:

jwatwatson@gmail.com (JAW)

†These authors contributed
equally to this work

‡These authors also contributed
equally to this work

9 ¹Mahidol Oxford Tropical Medicine Research Unit, Faculty of Tropical Medicine, Mahidol
10 University, Bangkok, Thailand; ²Centre for Tropical Medicine and Global Health, Nuffield
11 Department of Medicine, University of Oxford, United Kingdom; ³KEMRI-Wellcome
12 Trust Research Programme, Centre for Geographic Medicine Research-Coast, Kilifi
13 80108, Kenya; ⁴The Wellcome Sanger Institute, Cambridge, United Kingdom; ⁵Wellcome
14 Trust Centre for Human Genetics, University of Oxford, Oxford, United Kingdom;
15 ⁶Medical Research Council Clinical Trials Unit, University College London, United
16 Kingdom; ⁷Institute of Global Health Innovation, Imperial College, London, United
17 Kingdom; ⁸Nuffield Department of Medicine, University of Oxford, United Kingdom;
18 ⁹Department of Statistics, University of Oxford, United Kingdom

20 **Abstract**

21 Severe falciparum malaria has substantially affected human evolution. Genetic association
22 studies of patients with clinically defined severe malaria and matched population controls have
23 helped characterise human genetic susceptibility to severe malaria, but phenotypic imprecision
24 compromises discovered associations. In areas of high malaria transmission the diagnosis of
25 severe malaria in young children and, in particular, the distinction from bacterial sepsis, is
26 imprecise. We developed a probabilistic diagnostic model of severe malaria using platelet and
27 white count data. Under this model we re-analysed clinical and genetic data from 2,220 Kenyan
28 children with clinically defined severe malaria and 3,940 population controls, adjusting for
29 phenotype mis-labelling. Our model, validated by the distribution of sickle trait, estimated that
30 approximately one third of cases did not have severe malaria. We propose a data-tilting
31 approach for case-control studies with phenotype mis-labelling and show that this reduces false
32 discovery rates and improves statistical power in genome-wide association studies.

33

34 **Introduction**

35 Severe malaria caused by the parasite *Plasmodium falciparum* kills nearly half a million children
36 each year, mostly in sub-Saharan Africa (*World Health Organization, 2020*). By causing death in
37 children before they reach their reproductive age, *P. falciparum* has exerted a substantial selec-
38 tive evolutionary pressure on the human genome (*Carter and Mendis, 2002; Kariuki and Williams,*
39 *2020*). Recent advances in whole genome sequencing and haplotype imputation (*Teo et al., 2010*),

40 combined with data gathered prospectively from large patient cohorts has improved our under-
41 standing of genetic susceptibility to *P. falciparum* infection and severe disease (*Band et al., 2013*;
42 *The Malaria Genomic Epidemiology Network, 2014*; *Band et al., 2019*; *Leffler et al., 2017*) but many
43 questions remain unanswered (*Kariuki and Williams, 2020*). A major limitation of genetic associa-
44 tion studies in severe malaria is that the diagnosis of severe falciparum malaria in children is
45 imprecise (*White et al., 2013*; *Taylor et al., 2004*; *Bejon et al., 2007*). This imprecision increases
46 with transmission intensity because of the low positive predictive value of a 'positive blood film'
47 or rapid diagnostic test (RDT) in areas where the background prevalence of microscopy detectable
48 parasitaemia in apparently healthy young children is high (often around 30%, *Rodriguez-Barrquer*
49 *et al. (2018)*, but can exceed 90%, *Smith et al. (1994)*).

50 Severe falciparum malaria has been defined by experts convened by the World Health Organi-
51 zation (WHO) as clinical or laboratory evidence of vital organ dysfunction in the presence of circu-
52 lating asexual *P. falciparum* parasitaemia (*World Health Organisation, 2014*). The WHO definition
53 of severe malaria is aimed primarily at clinicians and health care workers managing patients with
54 malaria who appear severely ill. This appropriately prioritises sensitivity over specificity (*Anstey*
55 *and Price, 2007*). An inclusive clinical definition ensures that cases are not missed and patients
56 receive the best treatment. In contrast genetic association studies require high specificity (*Zonder-*
57 *van and Cardon, 2007*). For a given sample size, their statistical power, false-discovery rates and
58 the validity of their interpretation are weakened by phenotypic inaccuracy. Specificity in the diag-
59 nosis of severe malaria depends in part on the prevalence of malaria parasitaemia. This reflects
60 background transmission intensity. In areas of low or seasonal transmission (e.g. most of endemic
61 Asia and the Americas), clinical and laboratory signs of severity accompanied by a positive blood
62 film for *P. falciparum* are highly specific for severe malaria, which predominantly affects young
63 adults. In contrast in high transmission areas in sub-Saharan Africa and in lowland areas of the
64 island of New Guinea, where severe malaria is largely a disease of young children, the diagnostic
65 criteria for defining severe malaria are less specific because of the high background prevalence
66 of asymptomatic parasitaemia and the lower specificity of the clinical manifestations. Standard
67 case definitions of severe malaria will therefore inevitably include both patients with non-malarial
68 severe illness with concomitant parasitaemia, and with concomitant non-severe malaria.

69 Our goal was to develop a biomarker-based model that can differentiate probabilistically be-
70 tween 'true severe malaria' and severe illness not caused primarily by malaria, but with concomi-
71 tant parasitaemia. We define 'true severe malaria' conceptually as a febrile illness caused by malaria
72 parasites, with organ dysfunction, that can result in death whereby mortality is attributable directly
73 to the malaria parasites. This attributable mortality can be given a formal causal definition by us-
74 ing a conceptual (albeit unethical) randomised experiment of delayed versus prompt anti-malarial
75 therapy. In a theoretical patient population with true severe malaria, delay in administration of an
76 effective antimalarial would result in increased mortality (*Warrell et al. (1982)*; *Gomes et al. (2009)*,
77 whereas in a population with severe illness not caused by malaria ('not severe malaria') there would
78 not be a corresponding increase in mortality.

79 We developed a probabilistic diagnostic model of severe malaria based on haematological
80 biomarkers using data from 1,704 adults and children mainly from low transmission settings whose
81 diagnosis of severe malaria is considered to be highly specific. We used this model to demonstrate
82 low phenotypic specificity in a cohort of 2,220 Kenyan children who were diagnosed clinically with
83 severe malaria. We validated the predictions using a natural experiment, the distribution of sickle
84 cell trait (HbAS), the genetic polymorphism with the strongest known protective effect against all
85 forms of clinical malaria (*The Malaria Genomic Epidemiology Network, 2014*). Building on work
86 on 'data-tilting' (*Nie et al., 2013*), we suggest a new method for testing genetic associations in the
87 context of case-control studies in which cases are re-weighted by the probability that the severe
88 malaria diagnosis is correct under the model. As proof-of-concept, we ran a genome-wide associa-
89 tion study across 9.6 million imputed bi-allelic variants using the subset of cases with genome-wide
90 genotype data ($n = 1,297$) and population controls ($n = 1,614$). Adjusting for case mis-classification

decreased genome-wide false-discovery rates (*Storey, 2002*), and increased effect sizes in three of the top regions of the human genome most strongly associated with protection from severe malaria in East Africa (*HBB, ABO*, and *FREM3*, *Band et al., 2019*). A re-analysis of 120 directly typed polymorphisms in 70 candidate malaria-protective genes in the 2,220 Kenyan cases and 3,940 population controls, examining differential effects between correctly and incorrectly classified cases, suggests that the protective effect of glucose-6-phosphate dehydrogenase (G6PD) deficiency has been obscured in this population by case mis-classification. Our results show that adding full blood count meta-data - routinely measured in most hospitals in sub-Saharan Africa - to severe malaria cohorts would lead to more accurate quantitative analyses in case-control studies and increased statistical power.

Results

Reference model of severe malaria

We used the joint distribution of platelet counts and white blood cell counts (both on a logarithmic scale) to develop a simple biomarker-based reference model of severe malaria. To fit the reference model (i.e. $P[\text{Data} \mid \text{Severe malaria}]$), we used platelet and white count data from (i) severe malaria patient cohorts enrolled in low transmission areas where severe disease accompanied by a positive blood stage parasitaemia has a high positive predictive value for severe malaria (930 adults from Vietnam (*Hien et al., 1996*; *Phu et al., 2010*) and 653 adults and children from Thailand and Bangladesh); and (ii) severely ill African children with plasma *PfHRP2* concentrations $> 1,000$ ng/ml and $> 1,000$ parasites per μL of blood (121 children from Uganda, *Maitland et al., 2011*). Severe illness accompanied by a high plasma *PfHRP2* concentration makes the diagnosis of severe falciparum malaria highly specific (*Hendriksen et al., 2012*). The joint distribution of platelet and white blood cell counts in severe malaria was modelled as a bivariate *t*-distribution with both blood count variables on the \log_{10} scale.

Figure 1A shows the reference data (green triangles: patients with a highly specific diagnosis of severe malaria, summarised in Table 1) alongside data from a large Kenyan cohort of hospitalised children diagnosed with severe malaria, whose diagnosis had unknown specificity (pink squares). The median platelet count in the reference data was 57,000 per μL and the median total white blood cell count was 8,400 per μL . In contrast, the median platelet count in the Kenyan children was 120,000 per μL and the median total white blood cell count was 13,000 per μL . Direct comparisons of white counts across these two data sets are confounded by geography and age. Total white blood cell counts are known to be age-dependent and vary across genetic backgrounds, in particular lower neutrophil counts are associated with mutations in the *ACKR1* gene that results in the Duffy negative phenotype prevalent in African populations (*Reich et al., 2009*). However, after adjustment for age (see Methods), the marginal distributions of total white counts were comparable between Asian adults and children with severe malaria and African children with high plasma *PfHRP2* (Appendix 1). Platelet counts are not age dependent and do not vary substantially across genetic backgrounds. The marginal distributions of platelet counts were comparable between Asian adults and children with severe malaria and African children with high plasma *PfHRP2* (Appendix 1). A low platelet count (thrombocytopenia) is a universal feature of severe malaria (see evidence collated in Methods). To illustrate this important point, in a cohort of 566 severely ill Ugandan children enrolled in the FEAST trial (*Maitland et al., 2011*, a trial including all severe illness not restricted to severe malaria), low platelet counts were highly predictive of blood stage parasitaemia and elevated *PfHRP2* ($p=10^{-16}$ for a spline term on the \log_{10} platelet count in a generalised additive logistic regression model predicting $PfHRP2 > 1,000$ ng/mL, Appendix 2). Children enrolled in the FEAST trial who had significant thrombocytopenia ($<100,000$ platelets per μL) had comparable *PfHRP2* concentrations to Asian adults diagnosed with severe falciparum malaria (Figure 1B).

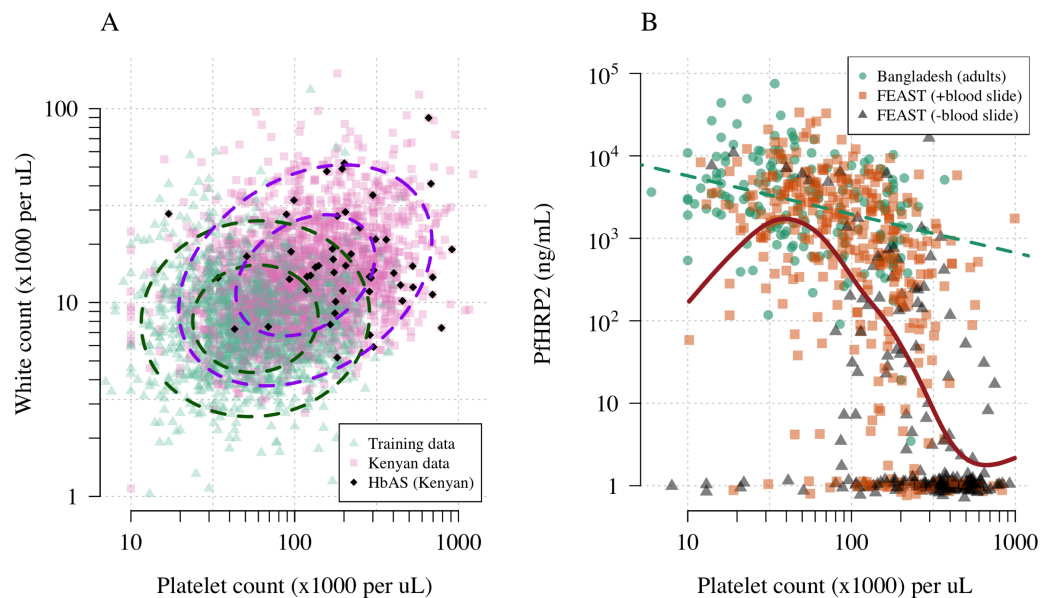


Figure 1. Platelet counts and white blood cell counts as diagnostic predictors of severe falciparum malaria. Panel A shows the bi-variate marginal distribution for the reference data (thought to be highly specific to severe malaria, green triangles, $n = 1,704$, summarised in Table 1) and for the Kenyan case data (pink squares, $n = 2,220$; black diamonds: HbAS). The dashed ellipses show the 50 and 95% bivariate normal probability contours approximating each dataset (dark green: training data; purple: Kenyan data). Panel B shows the relationship between platelet counts and plasma *Pf*HRP2 in adults with severe malaria from Bangladesh (green circles, $n = 172$, the dashed green line shows a linear fit) and in children enrolled in the FEAST trial ($n = 567$, not specific to severe malaria, *Maitland et al., 2011*). Undetectable plasma *Pf*HRP2 concentrations were set to 1 ng/mL \pm random jitter. Orange squares: malaria-positive blood slide; black triangles: malaria-negative blood slide. The brown line shows a spline fit to the FEAST data (*smooth.spline* function in R with default parameters) including the data points where *Pf*HRP2 was below the lower limit of detection.

Table 1. Summary of severe disease data sets used in our analyses. For age and parasite density we show the median values as the distributions are highly skewed. *For the FEAST trial, the severe malaria reference data set only included platelet and white count data from the 121 patients who had *PfHRP2* >1,000 ng/mL and >1,000 parasites per μ L.

	Bangladesh-Thailand	Vietnam	FEAST (Uganda)	Kenya
Description	Observational studies of severe malaria	Randomised controlled trials in severe malaria	Randomised controlled trial in severe febrile illness	Observational severe malaria cohort
Purpose	Reference data	Reference data	Reference data* and Fig 1B	Testing data
Published references	<i>Leopold et al.</i> (2019)	<i>Hien et al.</i> (1996); <i>Phu et al.</i> (2010)	<i>Maitland et al.</i> (2011)	<i>Ndila et al.</i> (2018)
n	653	930	567	2,220
Age (years, range)	28 (2-80)	30 (15-79)	2.1 (0-12)	2.3 (0-13)
Parasite density (per μ L, IQR)	48,984 (8,289-187,395)	83,084 (13,047-316,512)	400 (0-53,200)	72,000 (6,208-315,250)
Mortality (%)	18.2	12.9	11.3	11.6

139 Estimating the proportion of children mis-diagnosed with severe malaria

140 We can consider the hospitalised Kenyan children in this series as a mixture of two latent sub-
141 populations, 'severe malaria' and 'not severe malaria' (i.e an alternative aetiology for severe illness).
142 To estimate the proportion of each we use the distribution of HbAS, the human polymorphism
143 most protective against all forms of clinical falciparum malaria. HbAS provides at least 90% protec-
144 tion against severe malaria (*Taylor et al., 2012; The Malaria Genomic Epidemiology Network, 2014*).
145 The causal SNP rs334 was genotyped in 2,213 of the Kenyan children, of whom 57 were HbAS. The
146 causal pathways (a) or (b) in Figure 2 (note all children have been selected into the study on the
147 basis of clinical symptoms consistent with severe malaria) show how the distribution of HbAS can
148 be used to infer the marginal probability P(Severe malaria) in the Kenyan cohort as the prevalence
149 of HbAS is expected to differ in the two latent sub-populations.

150 We assumed that cases with the highest likelihood values P(Data | Severe malaria) under the
151 reference model (a bivariate *t*-distribution fit to the severe malaria reference data) had a diagnosis
152 of severe malaria that was 100% specific (top 40% of cases, a sensitivity analysis varied this thresh-
153 old). The cases with lower likelihood values were assumed to be drawn from a mixture of the two
154 latent populations with an unknown mixing proportion; the prevalence of HbAS in the 'not-severe
155 malaria' subgroup was estimated from a cohort of hospitalised children enrolled in the same hos-
156 pital and who were malaria blood slide positive but were clinically diagnosed as not having severe
157 malaria ($n = 6,748$ of whom 364 were HbAS (*Uyoga et al., 2019*)). We assumed that this diagnosis
158 of 'not-severe malaria' was 100% specific. Under these assumptions, we estimated that P(Severe
159 malaria)=0.64 (95% credible interval (C.I.) 0.46 to 0.8), implying that approximately one third of the
160 2,200 cases are from the 'not-severe malaria' sub-population (they have malaria parasitaemia in
161 addition to another severe illness - likely to be bacterial sepsis - Figure 2).

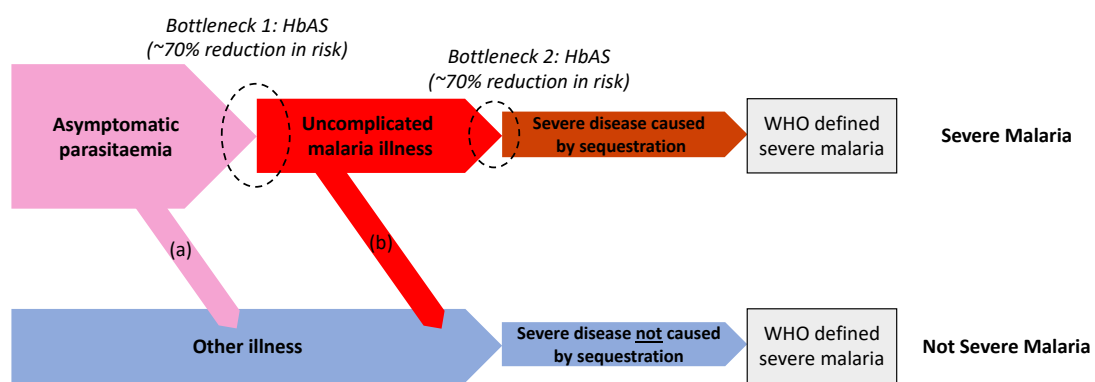


Figure 2. Theoretical causal pathways that lead to the clinical diagnosis of severe malaria under the current WHO definition (World Health Organisation, 2014). Pathways (a) & (b) represent the two ways patients can be mis-classified as severe malaria. For both pathways (a) & (b), we expect a higher prevalence of HbAS relative to the population with true severe malaria as a consequence of the protective bottlenecks. In this causal model we assume that HbAS does not protect against asymptomatic parasitaemia, although this assumption is not strictly necessary. Adapted with permission from *Small et al. (2017)*.

162 **Estimating individual probabilities of severe malaria**

163 We then estimated $P(\text{Severe malaria} \mid \text{Data})$ for each Kenyan case by fitting a mixture model to the
164 training data and to the Kenyan data jointly. The model assumed that the platelet and white count
165 data for the Kenyan children were drawn from a mixture of $P(\text{Data} \mid \text{Severe malaria})$ and $P(\text{Data} \mid$
166 $\text{Not severe malaria})$. The training data (Asian adults and children with severe malaria and African
167 children with $Pf\text{HRP}2 > 1,000 \text{ ng/mL}$) were assumed to be drawn only from $P(\text{Data} \mid \text{Severe malaria})$.
168 $P(\text{Data} \mid \text{Not severe malaria})$ was modelled itself as a mixture of bivariate t -distributions. We used
169 an informative prior on the mixture proportion ('severe malaria' versus 'not severe malaria') in the
170 Kenyan cases, a beta distribution approximating the posterior estimate from the analysis of HbAS
171 prevalence.

172 Figure 3A shows the bi-modal distribution of the posterior individual estimates of $P(\text{Severe}$
173 $\text{malaria} \mid \text{Data})$. As expected, the individual posterior probabilities of severe malaria were highly
174 predictive of HbAS ($p = 10^{-6}$ from a generalised additive logistic regression model fit, Figure 3C).
175 The individual probabilities were also predictive of in-hospital mortality ($p = 10^{-9}$ from a gener-
176 alised additive model fit; Figure 3D), and admission peripheral blood parasite density ($p = 10^{-25}$
177 from a generalised additive model fit; Figure 3E). In the top quintile of patients with the highest
178 estimated $P(\text{Severe malaria} \mid \text{Data})$, the prevalence of HbAS was 0.7% (3 out of 446). In contrast,
179 for patients in the lowest quintile of estimated $P(\text{Severe malaria} \mid \text{Data})$, the prevalence of HbAS
180 was 4.8% (21 out of 446). The patients with a low probability of severe malaria had a substantially
181 higher case fatality ratio (18.8% mortality for patients in the bottom quintile of $P(\text{Severe malaria} \mid$
182 $\text{Data})$ versus 6.1% mortality for the top quintile of $P(\text{Severe malaria} \mid \text{Data})$). This may be explained
183 by the higher case-specific mortality of severe bacterial sepsis (the most likely alternative cause of
184 severe illness). The admission parasite densities in patients with a probability of severe malaria
185 close to 1 were approximately five-fold higher than in patients with a probability of severe malaria
186 close to zero. The blood culture positive rate was 2.1% in the top quintile of $P(\text{Severe malaria} \mid$
187 $\text{Data})$, and 4.4% in the lowest quintile of $P(\text{Severe malaria} \mid \text{Data})$ and the individual probabilities
188 were predictive of blood culture results ($p = 0.004$ under a generalised additive logistic regression
189 model fit).

190 **Accounting for case imprecision in case-control studies**

191 'False-positive' cases reduce statistical power and dilute effect size estimates in case-control studies.
192 We propose a novel approach for case-control studies with phenotypic imprecision based on data
193 tilting (*Nie et al., 2013*). The idea is to 'tilt' the cases towards a pseudo-population with higher

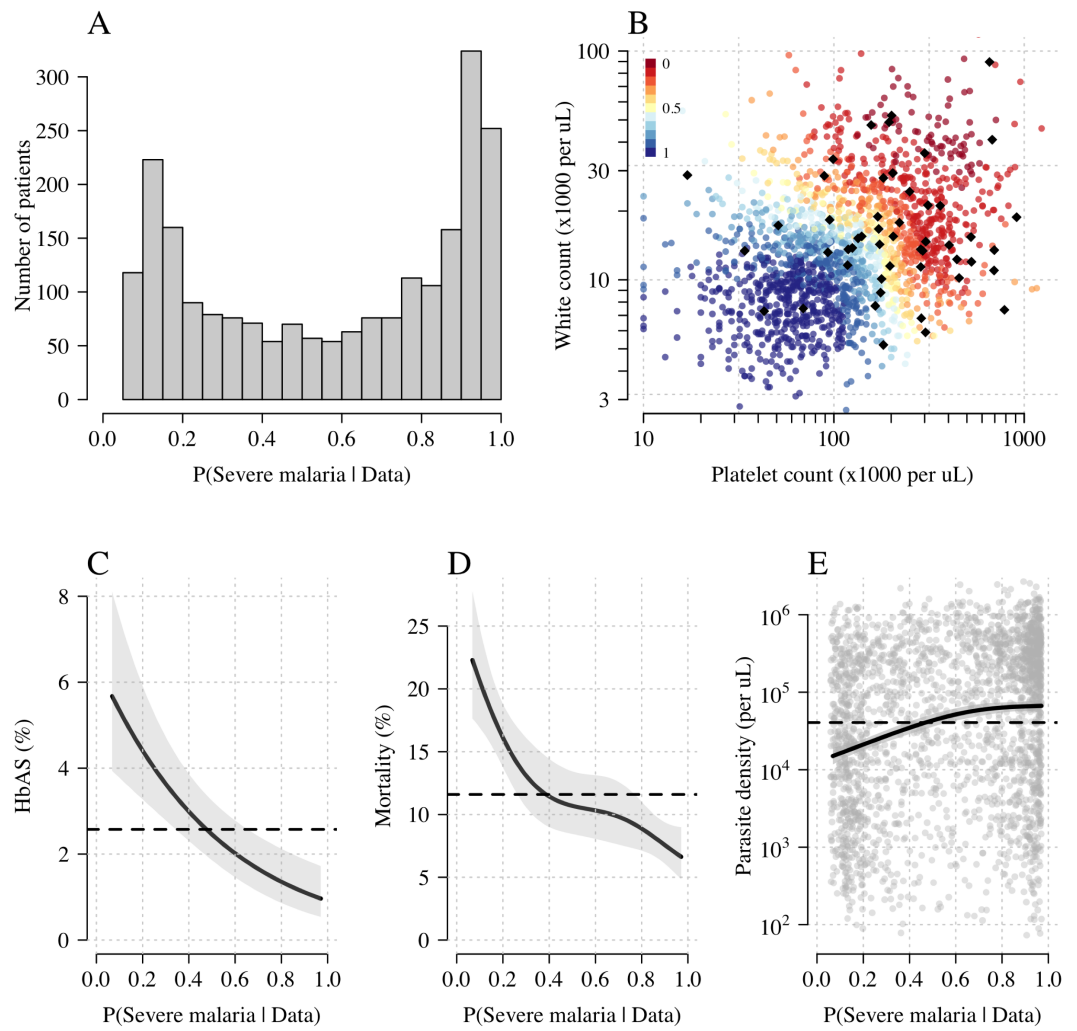


Figure 3. Model estimates of $P(\text{Severe malaria} | \text{Data})$ in 2,220 Kenyan children clinically diagnosed with severe malaria. Panel A: distribution of posterior probabilities of severe malaria being the correct diagnosis. Panel B shows these same probabilities plotted as a function of the platelet and white counts on which they are based (dark red: probability close to 0; dark blue: probability close to 1). The black diamonds show the HbAS individuals. Panels C-E show the relationship between the estimated probabilities of severe malaria and HbAS, in-hospital mortality, and admission parasite density, respectively. The black lines (shaded areas) show the mean estimated values (95% confidence intervals) from a generalised additive logistic regression model with a smooth spline term for the likelihood (R package *mgcv*). The horizontal lines in panels C-E show the mean values in the data.

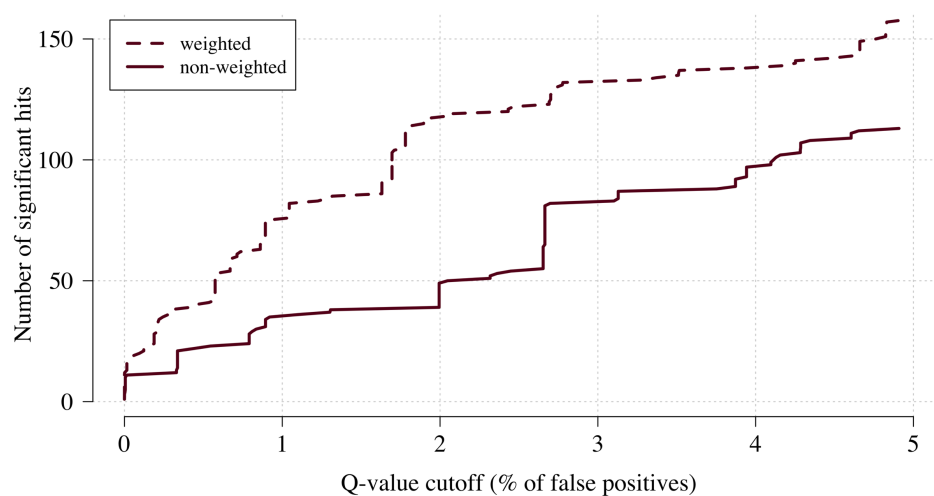


Figure 4. The number of significant hits as a function of the false discovery rate for the genome-wide association study across 9.6 million bi-allelic variants. This analysis is based on a subset of the Kenyan children with whole genome data available and passing quality checks $n=1,297$, and $n=1,614$ controls. Dashed line: weighted-model; thick line: non-weighted model.

194 specificity for severe malaria. We can do this by re-weighting the data by the probabilities $P(\text{Severe}$
195 malaria | Data), i.e. re-weighting the contribution to the log-likelihood in an association model.

196 We applied this approach as proof-of-concept to a genome-wide association study using the
197 subset of Kenyan children who had clinical and genome-wide data available (after quality control
198 checks $n=1,297$ cases) and a set of matched population controls ($n=1,614$), across 9.6 million bi-
199 allelic variants on the autosomal chromosomes (Band *et al.*, 2019). We compared the data-tilting
200 method to the standard non-weighted approach by estimating local false discovery rates (FDR,
201 Storey, 2002). Compared to the standard non-weighted GWAS, data-tilting substantially increased
202 the number of significant associations for local FDRs in the range of 1-5% (Figure 4). For example,
203 at an FDR of 2%, the number of significant hits is more than doubled with the additional hits all
204 around known loci associated with protection from severe malaria. We note that if the data weights
205 were not predictive of the true latent phenotype, we would expect fewer significant hits for a given
206 FDR because of the reduction in effective sample size. This is demonstrated by permuting the data
207 weights (for the cases only), which results in 50-75% reduction in the number of significant hits at
208 FDRs <5% (Appendix 3).

209 Examining three major genetic regions strongly associated with protection from severe malaria
210 in East Africa (*HBB*: HbAS; *ABO*: O blood group; *FREM3*: in close linkage with the GYPA/B/E structural
211 variants that encode the Dantu blood group; Band *et al.*, 2019), the data-tilting approach estimated
212 larger effect sizes compared to the non-weighted model in all three regions (effect size increases:
213 30% around *HBB*, 9% around *ABO*, and 5% around *FREM3*). This resulted in larger $-\log_{10}$ p-values
214 for *HBB* and *ABO*, but slightly smaller for *FREM3* (Figure 5). We note that there was no signal of
215 association at *ATP2B4* in this subset, most likely due to limited power (*ATP2B4* had the third largest
216 Bayes factor for association in the largest multi-center GWAS to date, Band *et al.*, 2019)).

217 **Reappraisal of directly typed polymorphisms**

218 We re-analysed case-control associations for 120 polymorphisms on 70 candidate malaria-protective
219 genes which were typed directly in the 2,220 Kenyan children along with 3,940 population controls.
220 In this case-control cohort, 14 polymorphisms had previously been identified as associated with
221 protection or increased risk in severe malaria (Ndila *et al.*, 2018). A re-analysis of these 14 variants

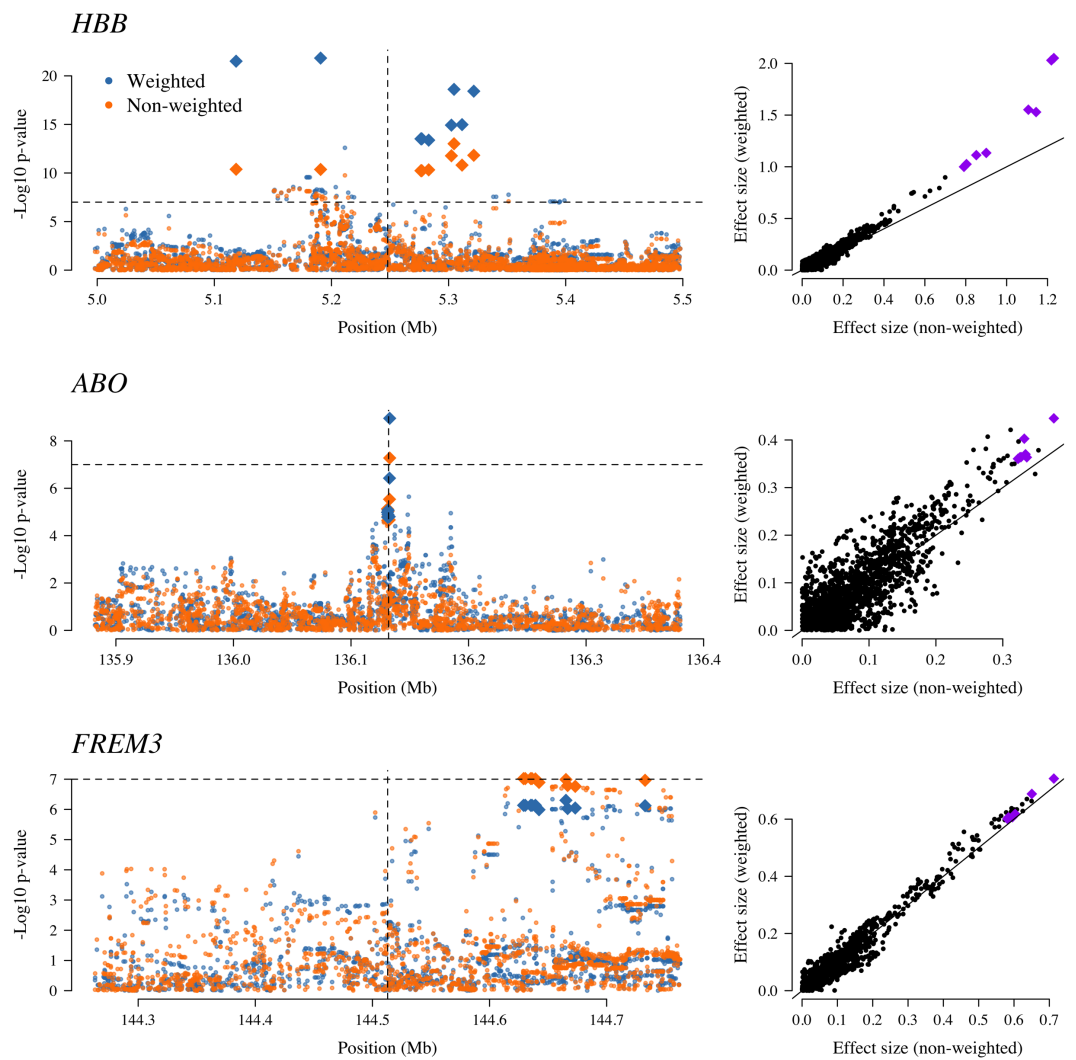


Figure 5. The three regions in the human genome with the greatest evidence for protection against severe malaria in East Africa (*HBB*, *ABO* and *FREM3*, Band et al., 2019). The Manhattan plots (left panels) compare p-values from the weighted model (blue) and the non-weighted model (orange). Each Manhattan plot is centred around the known causal position shown by the vertical dashed line (0.5 Mb region). The horizontal dashed line shows $p = 10^{-7}$ (threshold often used for defining genome-wide significance). The 10 positions with the greatest $-\log_{10}$ p-values under the non-weighted model are shown as large diamonds. The scatter plots on the right compare absolute effect size estimates under both models with the same top 10 hits shown by the larger purple diamonds. Increases of 30%, 9% and 5% are seen for the ten top hits for *HBB*, *ABO*, and *FREM3*, respectively.

222 using the same models of association as previously published and down-weighting the likely mis-
223 classified cases replicated the majority of associations, with increased effect sizes and increased
224 $-\log_{10}$ p-values (Appendix 4). For the three major genes (*HBB*, *ABO*, *FREM3*), effect sizes were in-
225 creased by 10-30% and associations all had higher significance levels on the $-\log_{10}$ scale (0.25-1.7).
226 The allele frequencies of all three polymorphisms were directly associated with the probability
227 weights, showing increased protection in individuals more likely to have severe malaria (Appendix
228 5). Two polymorphisms on the genes *ARL14* and *LOC727982*, reported previously as associated with
229 protection in severe malaria (neither of which are related to red cells), showed decreased effect
230 sizes and $-\log_{10}$ p-values and are thus potentially spurious hits.

231 We explored whether there was evidence of differential effects in the Kenyan cases using $P[\text{Severe}$
232 $\text{malaria} \mid \text{Data}]$ to assign probabilistically each case to the 'severe malaria' versus 'not severe
233 malaria' sub-populations. We fitted a categorical logistic regression model predicting the latent sub-
234 population label versus control, where the latent case label was estimated from the weights shown
235 in Figure 3A. This resulted in approximately 1,279 cases in the 'severe malaria' sub-population and
236 941 cases in the 'not severe malaria' sub-population. Differential effects were tested by compar-
237 ing the estimated log-odds for the two sub-populations. After accounting for multiple testing, two
238 polymorphisms showed significant differential effects: rs334 (derived allele encodes haemoglobin
239 S, $p = 10^{-6}$) and rs1050828 (derived allele encodes *G6PD*+202T, $p = 10^{-3}$ in the model fit to females
240 only), see Figure 6. As expected, rs334 was associated with protection in both sub-populations
241 (*Scott et al., 2011; Uyoga et al., 2019*) but the effect was almost 8 times larger on the log-odds scale
242 in the 'severe malaria' sub-population relative to the 'not severe malaria' sub-population (odds-ratio
243 of 0.029 [95% C.I. 0.0088-0.094] in the 'severe malaria' population versus 0.63 [95% C.I. 0.48-0.83]
244 in the 'not severe malaria' population). For rs1050828 (*G6PD*+202T allele), approximately the same
245 absolute log-odds were estimated for both sub-populations but they had opposite signs. Under
246 an additive model in females, the rs1050828 T allele was associated with protection in the 'severe
247 malaria' sub-population (odds-ratio of 0.71 [95% C.I. 0.57-0.88]) but with increased risk in the 'not
248 severe malaria' sub-population (odds-ratio of 1.30 [95% C.I. 1.00-1.70]). The additive model includ-
249 ing both males and females was consistent with these opposing effects but significant only at a
250 nominal threshold ($p = 0.02$). Opposing effects across the two sub-populations is consistent with
251 the hypothesis that G6PD deficiency leads to a greater risk of being erroneously classified as se-
252 vere malaria as under the severe anaemia criterion (*Watson et al., 2019*, shown in more detail
253 in Appendix 5). Investigation of haemoglobin concentrations as a function of $P[\text{Severe malaria} \mid$
254 $\text{Data}]$ indicates that the mis-classified group is very heterogeneous, but with a larger proportion of
255 severe anaemia (<5 g/dL) relative to the correctly classified sub-population (Appendix 6).

256 Discussion

257 The clinical diagnosis of severe falciparum malaria in African children is imprecise (*Taylor et al.,*
258 *2004; Bejon et al., 2007; White et al., 2013*). Even with quantitation of parasite densities, specificity
259 is still imperfect (*Bejon et al., 2007*). In children with cerebral malaria (unroutable coma with
260 malaria parasitaemia), the most specific of the severe malaria clinical syndromes, post-mortem
261 examination revealed another diagnosis in a quarter of cases studied in Blantyre, Malawi (*Taylor*
262 *et al., 2004*). Diagnostic specificity can be improved by visualisation of the obstructed microcircula-
263 tion in-vivo (e.g. through indirect ophthalmoscopy) or from parasite biomass indicators (quantita-
264 tion and staging of malaria parasites on thin blood films, counting of neutrophil ingested malaria
265 pigment, measurement of plasma concentrations of *Pf*HRP2 or parasite DNA), but these are still
266 largely research procedures and have not been widely adopted or measured at scale for genetic
267 association studies. Our results suggest that imprecision in clinical phenotyping is more substan-
268 tial than thought previously. In this cohort of 2,220 Kenyan children diagnosed with severe malaria
269 from an area of moderate transmission, a probabilistic assessment suggests that around one third
270 may not have had severe malaria (although malaria may have contributed to their illness, *Small*
271 *et al., 2017*). This supports our previous conclusion that differences in treatment effects between

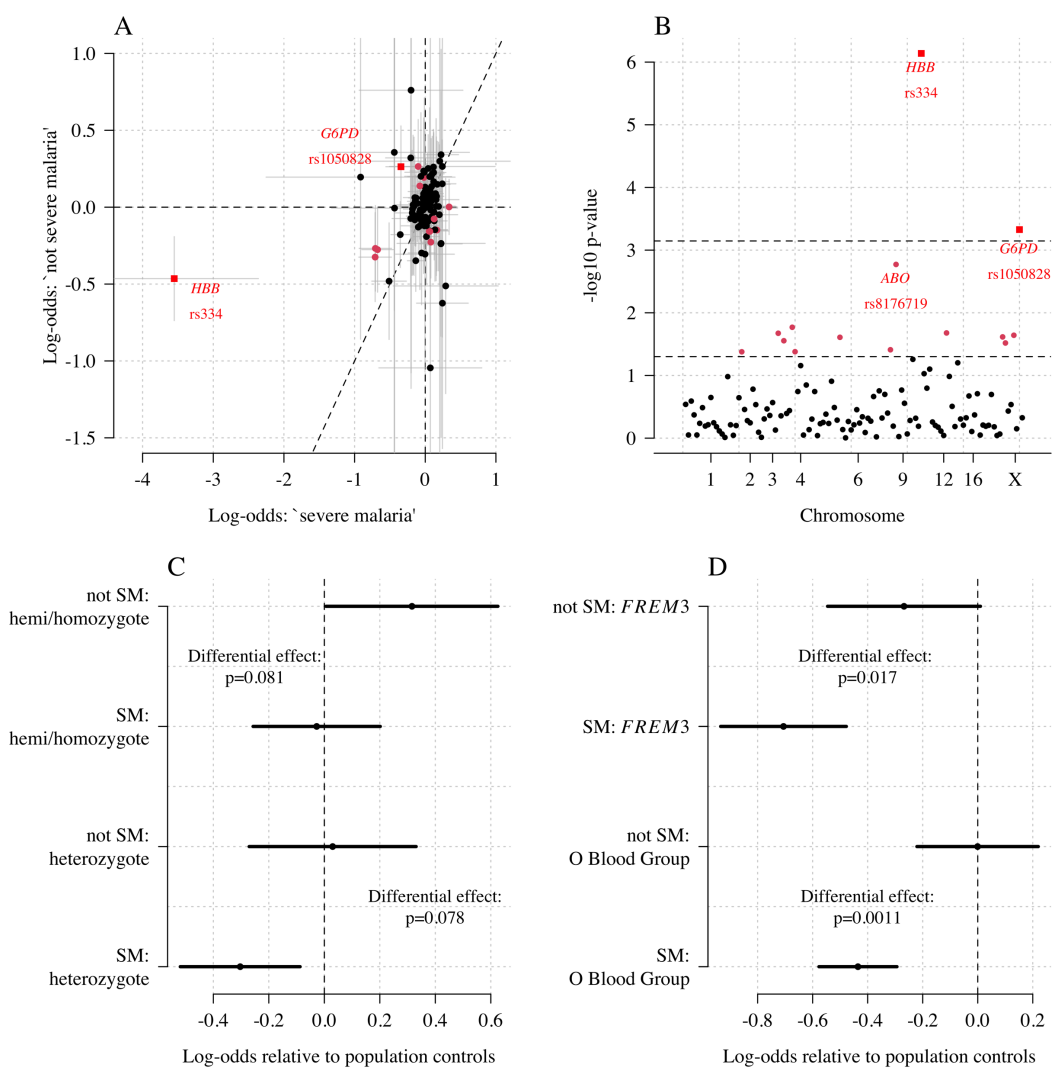


Figure 6. Exploring differential effects in 120 directly typed polymorphisms across 70 candidate malaria-protecting genes. Panel A: case-control effect sizes estimated for the 'severe malaria' sub-population versus the 'not severe malaria' sub-population ($n = 3,940$ controls and $n = 2,220$ cases, with approximately 1,279 in the 'severe malaria' sub-population and 941 in the 'not severe malaria' sub-population). The vertical and horizontal grey lines show the 95% credible intervals. Panel B shows the \log_{10} p-values testing the hypothesis that the effects are the same for the two sub-populations relative to controls. The top dashed line shows the Bonferroni corrected $\alpha = 0.05$ significance threshold (assuming 70 independent tests). The bottom dashed line shows the nominal $\alpha = 0.05$ significance threshold. In both panels, red circles denote $p < 0.05$ (nominal significance level), and red squares denote $p < 0.05/70$. Panel C: Analysis of the rs1050828 SNP (encoding G6PD+202T) under a non-additive model (hemi/homozygotes and heterozygotes are distinct categories). This shows that heterozygotes are clearly under-represented in the 'severe malaria' sub-population and hemi/homozygotes are clearly over-represented in the 'not severe malaria' sub-population. Panel D: evidence of differential effects for the O Blood Group (rs8176719, recessive model) and *FREM3* (additive model).

272 Asian adults and African children (i.e the benefits of artesunate over quinine in severe malaria
273 estimated from randomised trials, *Dondorp et al., 2005, 2010*) are predominantly driven by differ-
274 ences in diagnostic specificity (*Hendriksen et al., 2012; White et al., 2013*). Mortality was higher
275 in the severe 'not malaria' patients, probably because the main illness was bacterial sepsis. This
276 strongly supports current recommendations to give broad spectrum antibiotics to all children in
277 endemic areas with suspected severe malaria (*World Health Organisation, 2014*). Using HbAS as a
278 natural experiment to validate the biomarker model, we show that the joint distribution of platelet
279 and white blood cell counts is a diagnostic predictor of severe malaria. Complete blood counts are
280 inexpensive and increasingly available in low-resource setting hospitals. Application of an upper
281 threshold of 200,000 platelets per μL would have substantially decreased mis-classification in this
282 large cohort of Kenyan children diagnosed with severe malaria.

283 This re-analysis using rich clinical data provides additional evidence for the three major genetic
284 polymorphisms protective against severe malaria present in East Africa. After probabilistic down-
285 weighting of the likely mis-classified cases, substantial increases in effect sizes were found. Dilu-
286 tion of effect sizes resulting from mis-classification could explain the large heterogeneity in effects
287 noted in the largest severe malaria GWAS to date (*Band et al., 2019*). For haemoglobin S (rs334)
288 there was a 4-fold variation in estimated odds-ratios across participating sites. Some of this het-
289 erogeneity can be attributed to variations in linkage disequilibrium affecting imputation accuracy
290 (*Band et al., 2013*), but our analysis shows an additional substantial source of heterogeneity which
291 results from diagnostic imprecision. This can be adjusted for if detailed clinical data are available.
292 For example, in the case of rs334 (directly typed), the data-tilting approach results in a 25% increase
293 in effect size on the log-odds scale, corresponding to 35% decrease in estimated odds-ratios (0.1
294 versus 0.16).

295 As for the interpretation of genetic effects, one of the most interesting results concerns the
296 *G6PD* gene. *G6PD* deficiency is the most common enzymopathy of humans. Its potential role in
297 protecting against falciparum malaria has been controversial (*Clarke et al., 2017; Watson et al.,*
298 *2019*). A very large multi-country genetic association study with over 11,000 severe malaria cases
299 and 17,000 population controls found no overall protective effect of the *G6PD+202T* allele (the
300 most common mutation in sub-Saharan Africa causing *G6PD* deficiency), under an additive model
301 (*The Malaria Genomic Epidemiology Network, 2014*). The same pattern is observed in this Kenyan
302 cohort (which is a subset of the larger study). In the Kenyan cohort overall, a previous analysis
303 found no clear evidence of protection for male homozygotes but substantial evidence of protec-
304 tion for female heterozygotes (*Uyoga et al., 2015*). This would suggest a heterozygote advantage
305 leading to a balancing polymorphism. However, when the Kenyan cases are modelled as two dis-
306 tinct sub-populations, there is evidence of differential effects between the 'severe malaria' and 'not
307 severe malaria' sub-populations. Hemi and homozygous *G6PD* deficiency was associated with an
308 increased risk of mis-classification (reflecting an increased risk of severe anaemia), but it is unclear
309 whether or not hemi/homozygous *G6PD* deficiency was protective in the 'true severe malaria' sub-
310 population (Figure 6C). On the other hand, heterozygote deficiency was very clearly protective in
311 the true severe malaria subgroup, consistent with previous findings, and did not appear to lead
312 to an increased risk of mis-classification (consistent with a lower risk of extensive haemolysis and
313 thus false classification in heterozygotes who have both normal and *G6PD* deficient erythrocytes
314 in their circulation). When examining the 'severe malaria' sub-population only, the sample size in
315 this study is too small to discriminate between the heterozygote and additive models of associa-
316 tion. In our view, the relationship between *G6PD* deficiency and severe falciparum malaria remains
317 unanswered. A biomarker driven approach should be applied to other case-control cohorts for a
318 definitive understanding of the role of this major human polymorphism.

319 The limitations of our diagnostic model can be summarised as follows. First, the validity and
320 interpretation of the individual probabilities of severe malaria is heavily dependent on the refer-
321 ence model and thus the reference data. Our reference data were primarily from Asian adults in
322 whom diagnostic specificity for severe malaria is thought to be very high. Diagnostic checks sug-

323 gested that the marginal distributions of platelet counts were similar between adults and children,
324 and we made age corrections to the white blood cell count, but small deviations could reduce the
325 discriminatory value (e.g. lower white counts associated with the Duffy negative phenotype, *Reich*
326 *et al.*, 2009). Second, it is possible that rare genetic conditions exist in which the probabilities of
327 severe malaria under this model might be biased. One example is sickle cell disease (HbSS, <0.5%
328 in the Kenyan cases), which results in chronic inflammation with high white counts and low platelet
329 counts relative to the normal population (*Sadarangani et al.*, 2009). The 11 children with HbSS in
330 this cohort were all assigned low probabilities of severe malaria, but this should be interpreted
331 with caution. Whether HbSS is protective against severe malaria or increases the risk of severe
332 malaria remains unclear (*Williams and Obaro*, 2011). For these patients, other biomarkers such
333 as plasma *Pf*HRP2 may be more appropriate. Third, it is possible that the joint distribution of the
334 complete blood count variables used to fit the reference model could be dependent on the severe
335 malaria sub-phenotype. For example, if the reference data were biased towards cerebral malaria,
336 and the joint distribution of platelet and white cell counts in cerebral malaria differed from those
337 in the other severe malaria syndromes, then the predicted outliers could represent other forms
338 of severe malaria instead of 'not-severe' malaria. However, there are no known biological reasons
339 why this would be the case. The strong correlation between platelet counts and *Pf*HRP2 (Figure
340 1B) suggests that low platelet counts are a universal feature of severe malaria.

341 In summary, under a probabilistic model based on routine blood count data, we have shown
342 that it is possible to estimate mis-classification rates in diagnosed severe childhood malaria in a
343 malaria endemic area of East Africa and compute probabilistic weights that can downweight the
344 contribution of likely mis-classified cases. The well-established protective effect of HbAS provided
345 an independent validation of the model. Relative to predicted mis-classified cases, patients pre-
346 dicted to have 'true severe malaria' had a substantially lower prevalence of HbAS, higher parasite
347 densities, lower rates of positive blood cultures, and lower mortality. These data strongly sup-
348 port the current guideline to give broad spectrum antibiotics to all children with suspected severe
349 malaria and suggest that normal range platelet counts (>200,000 per μ L) could be used as a simple
350 exclusion criterion in studies of severe malaria. Based on this analysis we recommend that future
351 studies in severe malaria collect and record complete blood count data. Further studies of platelet
352 and white blood cell counts from a diverse cohort of children with severe falciparum malaria, con-
353 firmed using high specificity diagnostic techniques such as visualisation of the microcirculation,
354 and measurement of plasma *Pf*HRP2, or plasma *P. falciparum* DNA concentrations should be con-
355 ducted to validate this approach.

356 Methods and Materials

357 Data

358 Kenyan case-control cohort

359 The Kenyan case-control cohort has been described in detail previously (*Ndila et al.*, 2018). Severe
360 malaria cases consisted of all children aged <14 years who were admitted with clinical features
361 of severe falciparum malaria to the high dependency ward of Kilifi County Hospital between June
362 11th 1999 and June 12th 2008. Severe malaria was defined as a positive blood-film for *P. falciparum*
363 along with: prostration (Blantyre Coma Score of 3 or 4); cerebral malaria (Blantyre Coma Score
364 of <3); respiratory distress (abnormally deep breathing); severe anaemia (haemoglobin < 5 g/dL).
365 Controls were infants aged 3-12 months who were born within the same area as the cases and who
366 were recruited to a cohort study investigating genetic susceptibility to a wide range of childhood
367 diseases. Cases and controls were genotyped for the rs334 SNP and for α^+ -thalassaemia along with
368 120 other SNPs using DNA extracted from fresh or frozen samples of whole blood as described in
369 detail previously (*Ndila et al.*, 2018; *Wambua et al.*, 2006).

370 Fluid Expansion as Supportive Therapy (FEAST)

371 FEAST was a multicentre randomised controlled trial comparing fluid boluses for severely ill chil-
372 dren ($n = 3,161$) that was not specific to severe malaria (*Maitland et al., 2011*). Platelet counts, white
373 blood cell counts, parasite densities and *Pf*HRP2 were jointly measured for 566 children (patients
374 enrolled in the sites in Mulago, Lacor and Mbale, in Uganda). In order to select only those with a
375 very high probability of having severe malaria as the primary cause of illness, we selected the 121
376 children who had measured *Pf*HRP2 $> 1,000$ ng/mL and parasitaemia $> 1,000$ per μL .

377 AQ Vietnam and AAV randomised controlled trials

378 The AQ and the AAV studies were two randomised clinical trials in Vietnamese adults diagnosed
379 clinically with severe falciparum malaria recruited to a specialist ward of the Hospital for Tropical
380 Diseases, Ho Chi Minh City, Vietnam, between 1991 and 2003 (*Hien et al., 1996; Phu et al., 2010*). AQ
381 Vietnam was a double blind comparison of intramuscular artemether versus intramuscular quinine
382 ($n = 560$); AAV compared intramuscular artesunate and intramuscular artemether ($n = 370$).

383 Observational studies in Thai and Bangladeshi adults and children

384 We included data from multiple observational studies in severe falciparum malaria conducted by
385 the Mahidol Oxford Tropical Medicine Research Unit in Thailand and Bangladesh between 1980
386 and 2019. These pooled data have been described previously (*Leopold et al., 2019*). Platelet counts
387 and white blood cell counts were available in 657 patients. We excluded one 30 year old adult from
388 Bangladesh whose recorded platelet count was 1,000 per μL , and three other adults with platelet
389 counts greater than 450,000 per μL as outliers reflecting likely data entry errors. Plasma *Pf*HRP2
390 concentrations were available in 172 patients from Bangladesh. 55 patients from this series were
391 younger than 15 years of age.

392 **Multiple imputation**

393 In the Kenyan severe malaria cohort ($n = 2,220$), data on platelet counts were missing in 18%, white
394 blood counts were missing in 0.2%, and parasite density was missing in 1.6%. In-hospital outcome
395 (died/survived) was missing for 13 patients. rs334 genotype was missing for 7; α^+ -thalassaemia
396 genotype was missing for 101 patients. In the Vietnamese adults, platelet counts were missing in
397 4%, white counts in 2% and parasitaemia in 0%.

398 We did multiple imputation using random forests for all available clinical variables using the R
399 package *missForest* (targeted genotyping data was not included for imputation). Appendix 7 shows
400 the missing data pattern in the studies in Vietnamese adults and in the Kenyan severe malaria cases.
401 Ten datasets were imputed for each dataset independently and were used for the subsequent
402 analyses. Analyses using directly typed genetic polymorphisms or the within-hospital outcome as
403 the dependent variables used only the data where these outcomes were recorded, assuming that
404 they were missing at random.

405 **Reference model of severe malaria**

406 **Biological rationale**

407 Thrombocytopenia accompanied by a normal white blood count and a normal neutrophil count
408 are typical features of severe malaria (*Hanson et al., 2015; Leblanc et al., 2020*), but they may
409 also occur in some systemic viral infections and in severe sepsis. Neutrophil leukocytosis may
410 sometimes occur in very severe malaria, but is more characteristic of pyogenic bacterial infections.
411 These indices, whilst individually not very specific, could each have useful discriminatory value.
412 We reasoned therefore that their joint distribution could help discriminate between children with
413 severe malaria versus those severely ill with coincidental parasitaemia. The Kenyan severe malaria
414 cohort did not have differential white count data, so we used platelet counts and total white blood
415 cell counts as the two diagnostic biomarkers in the reference model of severe malaria.

416 Choice of training data and confounders

417 The best data for fitting the biomarker model are either from children or adults from low transmis-
418 sion areas (where parasitaemia has a high positive predictive value); or in children or adults with
419 high plasma *Pf*HRP2 measurements indicating a large latent parasite biomass (*Hendriksen et al.*,
420 2012).

421 In the first years of life, white blood cell counts are often much higher than in adults because of
422 lymphocytosis. We used data from 858 children from the FEAST trial, in whom white counts were
423 measured, to estimate the relationship between age and mean white count in severe illness (me-
424 dian age was 24 months). The estimated relationship is shown in Appendix 8 (using a generalised
425 additive linear model with the white count on the \log_{10} scale), with mean white counts reaching a
426 plateau around 5 years of age. We used this to correct all white count data in children less than 5
427 years of age, both in the training data and the Kenyan cohort.

428 There is also a systematic difference associated with the Duffy negative phenotype which is
429 near fixation in Africa but absent in Asia. Duffy negative individuals have lower neutrophil counts
430 (termed benign ethnic neutropenia) (*Reich et al.*, 2009). The use of Asian adults to estimate the
431 reference distribution of white counts in severe malaria could thus falsely include individuals with
432 elevated white counts (relative to the normal ranges). However, a diagnostic quantile-quantile plot
433 (Appendix 1, on the log-scale) comparing the white blood cell count distribution in Vietnamese
434 adults and in children in the FEAST trial who had *Pf*HRP2 > 1,000 ng/mL did not suggest any major
435 differences. In fact the African children had slightly higher white counts on average even after
436 the correction for age. This may represent imperfect specificity for severe malaria when using a
437 plasma *Pf*HRP2 cutoff of 1,000 mg/mL.

438 For platelet counts (which have the greatest diagnostic value for severe malaria in our series)
439 age is not a confounder and published data support the hypothesis that thrombocytopenia is highly
440 specific for 'true' severe malaria in children as well as adults suspected of having severe malaria
441 (with a diagnostic and a prognostic value). The French national guidelines specifically mention
442 thrombocytopenia (<150,000 per μ L) for the diagnosis of severe malaria in children who have trav-
443 elled to a malaria endemic area. In a French paediatric severe malaria series in travellers, almost
444 half had severe thrombocytopenia (<50,000 per μ L) (*Lanneaux et al.*, 2016; *Mornand et al.*, 2017).
445 In Dakar, Senegal (one of the lowest transmission areas in Africa) thrombocytopenia was an in-
446 dependent predictor of death and the median platelet count was 100,000 (*Gérardin et al.*, 2007,
447 2002). Comparison of the distributions of platelet counts (on the log scale) between Asian children
448 and Asian adults suggested no major differences (Appendix 1), although we had few data for Asian
449 children. In the seminal Blantyre autopsy study (*Taylor et al.*, 2004), platelet counts were substan-
450 tially different between fatal cases confirmed post-mortem to be severe malaria (62,000 per μ L,
451 and 56,000 per μ L for the children with sequestration only, and for sequestration + microvascular
452 pathology, respectively) and fatal cases with a mis-diagnosis of severe malaria (no sequestration:
453 176,000 per μ L; the inter-group difference was statistically significant, $p = 0.008$). A larger cohort
454 from the same centre in Malawi reported substantially higher platelet counts in retinopathy nega-
455 tive cerebral malaria (mean platelet count was 161,000 per μ L, $n = 288$) compared to retinopathy
456 positive cerebral malaria (mean count was 81,000 per μ L, $n = 438$) (*Small et al.*, 2017).

457 We visually checked approximate normality for each marginal distribution using quantile-quantile
458 plots (Appendix 9). On the \log_{10} scale, platelet counts and white counts show a good fit to the nor-
459 mal approximation but with some outliers so a *t*-distribution was used (robust to outliers). For all
460 modelling of the joint distribution of platelet counts and white blood cell counts, we chose bivariate
461 *t*-distributions with 7 degrees of freedom as the default model. The final reference model used was
462 a bi-variate *t*-distribution fit to the joint distribution of platelet counts and white counts both on
463 the logarithmic scale. On the \log_{10} scale the mean values (standard deviations) were approximately
464 1.76 (0.11) and 0.92 (0.055) for platelets and white counts, respectively. The covariance was approx-
465 imately 0.0035. These values varied very slightly across the ten imputed datasets. Log-likelihood

466 values for each severe malaria case in the Kenyan cohort were calculated for each imputed dataset
467 independently. The median log-likelihoods per case were then used in downstream analyses.

468 Limitations of the model

469 The diagnostic model of severe malaria using platelet counts and white blood cell counts cannot
470 be applied to all patients. We summarise here the known and possible limitations. When using this
471 model to estimate the association between a genetic polymorphism and the risk of severe malaria,
472 if the genetic polymorphism of interest affects the complete blood count independently, there will
473 be selection bias (see the directed acyclic graph in Appendix 10). One example is HbSS. Children
474 with HbSS have chronic inflammation with white blood cells counts about 2-3 times higher than
475 normal and slightly lower platelet counts (*Sadarangani et al., 2009*). All 11 children in the Kenyan
476 cohort with HbSS were assigned low probabilities of having severe malaria (Appendix 10), but these
477 probabilities could reflect a deficiency of the model. Including or excluding these children from the
478 analysis had no impact on the results as they represent less than 0.5% of the cases.

479 The second possible limitation concerns the validation using HbAS. Previous studies have sug-
480 gested negative epistasis between the malaria-protective effects of HbAS and α^+ -thalassaemia
481 (*Williams et al., 2005; Opi et al., 2014*). The 3.7 kb deletion across the *HBA1-HBA2* genes (known as
482 α^+ -thalassaemia) has an allele frequency of ~ 40% in this population, therefore 16% of HbAS individ-
483 uals are homozygous for α^+ -thalassaemia (*Ndila et al., 2020*). Negative epistasis implies that those
484 with both polymorphisms would have less or no protective effect against severe malaria. Of the
485 2,113 Kenyan cases with both HbS and α^+ -thalassaemia genotyped, 13 were HbAS and homozy-
486 gous α^+ -thalassaemia. Appendix 11 shows that the majority of those with both polymorphisms
487 had clinical indices pointing away from severe malaria suggesting that the observed number of
488 patients with both HbAS and homozygous α^+ -thalassaemia is inflated by 2 to 3 fold.

489 The third possible problem concerns the use of white blood cell counts in relation to invasive
490 bacterial infections. Bacteraemia could either be the cause of severe illness (with coincidental
491 parasitaemia), or it could be concomitant (which may result from extensive parasitised erythrocyte
492 sequestration in the gut), i.e. a result of severe malaria. The former should be identified as 'not-
493 severe malaria' (as bacteraemia is the main cause of illness), but the latter should be identified as
494 'severe malaria' and might be mis-classified as 'not-severe malaria' under our model. However, in
495 a series of 845 Vietnamese adults (high diagnostic specificity), only one of eight patients who had
496 concomitant invasive bacterial infections and a white count measured had leukocytosis (median
497 white count was 8,100; range 3,500 to 14,850 per μL , *Phu et al., 2020*).

498 Estimating the diagnostic specificity in the Kenyan cohort

499 We assume that the Kenyan cases are a latent mixture of two sub-populations: P_0 is the population
500 'severe malaria' and P_1 is the population 'not-severe malaria' (mis-classified). For a set of diagnostic
501 biomarkers X , this implies that $X \sim G = \pi f_0 + (1 - \pi) f_1$, where f_0, f_1 are the sampling distributions
502 (likelihoods) of each sub-population, respectively.

503 We can infer the value of π (proportion correctly classified as severe malaria) without mak-
504 ing parametric assumptions about f_1 by using the distribution of HbAS (motivated by the causal
505 pathways shown in Figure 2). This is done as follows: we first estimate \hat{f}_0 by fitting a bivariate t -
506 distribution to the training data - this approximates the sampling distribution for P_0 . We then make
507 three assumptions:

- 508 1. Out of the 2,213 Kenyan cases with rs334 genotyped, we assume that cases in the top 40th
509 percentile of the likelihood distribution under \hat{f}_0 are drawn from P_0 : $N_0 = 887$, of which
510 $N_0^{\text{sickle}} = 9$ are HbAS.
- 511 2. For the other cases the proportion drawn from P_0 is unknown and denoted π' : $N_G = 1,326$,
512 of which $N_G^{\text{sickle}} = 48$ are HbAS.
- 513 3. Finally, additional information is incorporated by using data from a cohort of individuals with
514 severe disease from the same hospital who had positive malaria blood slides but whose di-

515 agnosis was not severe malaria ($N_1 = 6,748$, of which $N_1^{sickle} = 364$ were HbAS) (*Uyoga et al., 2019*).
 516

Under these assumptions, we can fit a Bayesian binomial mixture model to these data with three parameters: $\{\pi', p_0, p_1\}$. The likelihood is given by:

$$\begin{aligned} N_0^{sickle} &\sim \text{Binomial}(p_0, N_0) \\ N_G^{sickle} &\sim \text{Binomial}(\pi' p_0 + (1 - \pi') p_1, N_G) \\ N_1^{sickle} &\sim \text{Binomial}(p_1, N_1) \end{aligned}$$

517 The priors used were: $p_1 \sim \text{Beta}(5, 95)$ (i.e. 5% prior probability with 100 pseudo observations);
 518 $p_0 \sim \text{Beta}(1, 99)$ (1% prior probability with 100 pseudo observations). A sensitivity analysis with
 519 flat beta priors ($\text{Beta}[1, 1]$) did not qualitatively change the result (by one percentage point for the
 520 final estimate of π). To check the validity of the use of the external population from *Uyoga et al.*
 521 (2019), we did a sensitivity analysis using the lowest quintile of the likelihood ratio distribution as
 522 a population drawn entirely from P_1 (instead of the external data from *Uyoga et al., 2019*).

523 **Estimating P(Severe malaria | Data) in the Kenyan cohort**

Denote the platelet and white count data from the FEAST trial as $\{X_i^{\text{FEAST}}\}_{i=1}^{121}$; the data from the Vietnamese adults and children as $\{X_i^{\text{Asia}}\}_{i=1}^{1583}$; the data from the Kenyan children as $\{X_i^{\text{Kenya}}\}_{i=1}^{2220}$. We fit the following joint model to the training biomarker data and the Kenyan biomarker data.

$$\begin{aligned} X_i^{\text{FEAST}} &\sim \text{Student}(\mu_{SM}^1, \Sigma_{SM}^1, 7) \\ X_i^{\text{Asia}} &\sim \text{Student}(\mu_{SM}^2, \Sigma_{SM}^2, 7) \\ X_i^{\text{Kenya}} &\sim \pi f_0 + (1 - \pi) f_1 \\ f_0 &= p \text{Student}(\mu_{SM}^1, \Sigma_{SM}^1, 7) + (1 - p) \text{Student}(\mu_{SM}^2, \Sigma_{SM}^2, 7) \\ f_1 &= \sum_{j=1}^K \alpha_j \text{Student}(\mu_{notSM}^j, \Sigma_{notSM}^j, 7) \end{aligned}$$

with the following prior distributions and hyperparameters, where $\alpha = \{\alpha_1, \dots, \alpha_K\}$ such that $\sum_{j=1}^K \alpha_j = 1$:

$$\pi \sim \text{Beta}(40.3, 24.7)$$

$$p \sim \text{Beta}(2, 2)$$

$$\mu_{SM}^{1,2} \sim \text{Normal}(\{1.8, 0.95\}, 0.1^2)$$

$$\mu_{notSM}^{1..K} \sim \text{Normal}(\{2.5, 1.5\}, 0.25^2)$$

$$\alpha \sim \text{Dirichlet}(1/K, \dots, 1/K)$$

524 The covariance matrices $\Sigma_{SM}^{1,2}$ and $\Sigma_{notSM}^{1..6}$ were parameterised as their Cholesky LKJ decomposition,
 525 where the L correlation matrices had a uniform prior (i.e. hyperparameter $v=1$). The model was
 526 implemented in *rstan*.

527 This models the biomarker data in 'not severe malaria' as a mixture of K t -distributions. We
 528 chose $K = 6$ as the default choice (sensitivity analysis increasing this has no impact). The Dirichlet
 529 prior with hyperparameter $1/K$ forces sparsity in this mixture model (most of the prior weight is
 530 on the vertices of the K -dimensional simplex), see for example *Frühwirth-Schnatter and Malsiner-Walli (2019)*. This is a very general and flexible way of modelling the 'not severe malaria' distribution:
 531 we are not trying to make inferences about this distribution, we just want the mixture model to
 532 be flexible enough to describe it. The model also allows for differences in the joint distribution of
 533 platelet counts and white counts between the training datasets (FEAST trial and the Asian studies).
 534 The Kenyan cases drawn from the 'severe malaria' sub-population are then modelled as a mix of
 535 these two training models.

537 **Reweighted likelihood for case-control analyses**

538 For each $\{X_i^{\text{Kenya}}\}_{i=1}^{2220}$ we estimate the posterior probability of being drawn from the sampling dis-
539 tribution f_0 . The mean posterior probability then defines a precision weight w_i which can be used
540 in a standard generalised linear model (glm) with the same interpretation as inverse probability
541 weights. The weighted glm is equivalent to computing the maximum likelihood estimate where
542 the log-likelihood is weighted by w_i . In our case-control analyses all the controls are given weight
543 1. **Nie et al. (2013)** give a proof of correctness for this re-weighted log-likelihood (equivalent to
544 ‘tilting’ the dataset towards the desired distribution $\hat{f}_0(X)$). The log odds ratio computed from the
545 weighted logistic regression can be interpreted as the causal effect of the polymorphism on ‘true
546 severe malaria’ relative to the controls, where ‘true severe malaria’ is defined by the sampling dis-
547 tribution f_0 . Appendix 12 shows the results of a simulation study demonstrating how the effect
548 estimates and standard error estimates vary as a function of the proportion of mis-classified cases
549 (as given by the probability weights).

550 **Genome-wide association study**

551 Anonymised whole genome data from the Illumina Omni 2.5M platform for 1,944 severe malaria
552 cases and 1,738 population controls were downloaded from the European Genome-Phenome
553 Archive (dataset accession ID: EGAD00010001742, release date March 2019 (**Band et al., 2019**)).
554 This contained sequencing data on 2,383,648 variants. We used the quality control meta-data pro-
555 vided with the 2019 data release to select SNPs and individuals with high quality data. We first
556 excluded 386 individuals (due to relatedness: 155; missing data or low intensity: 226; gender: 5).
557 We then removed 616,426 SNPs that did not pass quality control, leaving a total of 1,767,222 SNPs.
558 We used plink2 to prune the SNPs (options: `-maf 0.01 -indep-pairwise 50 2 0.2`) down to a set of
559 462,120 SNPs in approximate linkage equilibrium. These SNPs were then used to calculate the
560 first 5 principal components (Appendix 13), which we subsequently used to control for population
561 structure in the genome-wide association study. We used the Michigan imputation server with the
562 1000 Genomes Phase 3 (Version 5) as the reference panel to impute 28.6 million polymorphisms
563 across the 22 autosomal chromosomes. This is a web-based service that runs imputation pipelines
564 (phasing is done with Eagle2, imputation with Minimac4). Encrypted results are returned with a one-
565 time password. Of the remaining 3,682 individuals (1,681 cases and 1,615 controls), we had clinical
566 data available for 1,297 cases. We only used the subset of individuals with clinical data available
567 in order for a fair comparison between the weighted and non-weighted genome-wide association
568 studies. We ran subsequent genome wide association studies on all bi-allelic sites with a minor al-
569 lele frequency $\geq 5\%$ (9,615,446 sites in total) assuming an additive model of association. We used
570 the R function `glm` with a binomial link for all tests of association (genetic data are encoded as the
571 number of reference alleles). The supplementary appendix gives the R code for weighted logistic
572 regression. The point estimates from the weighted model estimated by `glm` are correct but it is
573 necessary to transform the standard errors in order to take into account the reduction in effective
574 sample size (see code).

575 **Case-control study in directly typed polymorphisms**

576 We fit a categorical (multinomial) logistic regression model to the case-control status as a function
577 of the directly typed polymorphisms (120 after discarding those that are monomorphic in this pop-
578 ulation, see (**Ndila et al., 2018**) for additional details). We modelled the severe malaria cases as
579 two separate sub-populations with a latent variable: ‘severe malaria’ versus ‘not severe malaria’,
580 resulting in 3 possible labels (controls, ‘severe malaria’, ‘not severe malaria’). The models adjusted
581 for self-reported ethnicity and sex. The model was coded in `stan` (**Stan Development Team, 2020**)
582 using the log-sum-exp trick to marginalise out the likelihood over the latent variables (see code).
583 Normal(0,5) priors were set on all parameters and parameter estimates and standard errors were
584 estimated from the maximum a posteriori value (function `optimizing` in `rstan`).

585 **Code availability**

586 Code along with a minimal clinical dataset for reproducibility of the diagnostic phenotyping model
587 is available via a github repository: https://github.com/jwatowatson/Kenyan_phenotypic_accuracy.

588 **Data availability**

589 A curated minimal clinical dataset is currently available alongside the code on the github repository.
590 This will also be made available at publication via the KEMRI-Wellcome Harvard Dataverse (<https://dataverse.harvard.edu/dataverse/kwtrp>).

591 This paper used genome-wide genotyping data generated by *Band et al. (2019)*, available on
592 request from the European Genome-Phenome Archive (dataset accession ID: EGAD00010001742).

593 Requests for access to appropriately anonymized clinical data and directly typed genetic vari-
594 ants (*The Malaria Genomic Epidemiology Network, 2014*) for the Kenyan severe malaria cohort
595 can be made by application to the data access committee at the KEMRI-Wellcome Trust Research
596 Programme by e-mail to mmunene@kemri-wellcome.org.

597 The FEAST trial datasets are available from the principal investigator on reasonable request
598 (k.maitland@imperial.ac.uk). Requests for access to appropriately anonymized clinical data from
599 the AQ and AAV Vietnam study and the Asian paediatric cohort can be made via the Mahidol Oxford
600 Tropical Medicine Research Unit data access committee by emailing the corresponding author JAW
601 (jwatowatson@gmail.com) or Rita Chanviriyavuth (rita@tropmedres.ac).

602 **Acknowledgements**

603 This research was funded by The Wellcome Trust. A CC BY or equivalent licence is applied to the
604 author accepted manuscript arising from this submission, in accordance with the grant's open ac-
605 cess conditions. This work was done as part of SMAART (Severe Malaria Africa – A consortium for
606 Research and Trials) funded by a Wellcome Collaborative Award in Science grant (209265/Z/17/Z)
607 held in part by KM, NPJD and AD. TNW and NJW are senior and principal research fellows respec-
608 tively funded by the Wellcome Trust (202800/Z/16/Z and 093956/Z/10/C, respectively). ECG ac-
609 knowledges funding from a core grant to the MRC CTU at UCL from the MRC (MC_UU_12023/26)

610 The human data used in this study was generated through Malaria Genomic Epidemiology
611 Network Consortial Project 1, for which a full list of Consortium members is provided at <https://www.malariagen.net/projects/consortial-project-1/malariagen-consortium-members>.

612 The human data used in this study was generated through the Malaria Genomic Epidemiology
613 Network (<https://www.MalariaGEN.net>) Consortial Project 1, for which a full list of Consortium mem-
614 bers is provided at <https://www.malariagen.net/projects/consortial-project-1/malariagen-consortium-members>.
615 The Malaria Genomic Epidemiology Network study of severe malaria was supported by Wellcome
616 (WT077383/Z/05/Z) and the Bill & Melinda Gates Foundation (<https://www.gatesfoundation.org/>) through
617 the Foundations of the National Institutes of Health (<https://fnih.org/>) as part of the Grand Chal-
618 lenges in Global Health Initiative. The Resource Centre for Genomic Epidemiology of Malaria is sup-
619 ported by Wellcome (090770/Z/09/Z; 204911/Z/16/Z). This research was supported by the Medical
620 Research Council (G0600718; G0600230; MR/M006212/1). Wellcome also provides core awards
621 to the Wellcome Centre for Human Genetics (203141/Z/16/Z) and the Wellcome Sanger Institute
622 (206194).

623 This study also makes use of data from the FEAST trial. The FEAST trial was supported by a grant
624 (G0801439) from the Medical Research Council, United Kingdom provided through the (MRC) DFID
625 concordat. KM and ECG were supported by this grant.

626 **Author contributions**

627 JAW planned and conducted the analyses and wrote the paper. CMN, SU, AWM, MS, CN, NM, NP,
628 BT, SL, HK, KM, KR, NPJD, AD, PB, TNW, NJW contributed to data collection and data preparation.
629 JAW, NJW, CCH and TNW conceived and supervised the study. All authors read and approved the
630 final version of the paper.

633 **Competing interests**

634 None declared.

635 **References**

636 Anstey NM, Price RN. Improving case definitions for severe malaria. *PLoS Medicine*. 2007; 4(8):e267.

637 **Band G**, Le QS, Clarke GM, Kivinen K, Hubbart C, Jeffreys AE, Rowlands K, Leffler EM, Jallow M, Conway DJ, Sisay-Joof F, Sirugo G, d'Alessandro U, Toure OB, Thera MA, Konate S, Sissoko S, Mangano VD, Bougouma EC, Sirima SB, et al. Insights into malaria susceptibility using genome-wide data on 17,000 individuals from Africa, Asia and Oceania. *Nature Communications*. 2019; 10(1):5732. <https://doi.org/10.1038/s41467-019-13480-z>, doi: 10.1038/s41467-019-13480-z.

642 **Band G**, Le QS, Jostins L, Pirinen M, Kivinen K, Jallow M, Sisay-Joof F, Bojang K, Pinder M, Sirugo G, et al. 643 Imputation-based meta-analysis of severe malaria in three African populations. *PLoS Genetics*. 2013; 9(5):e1003509.

645 **Bejon P**, Berkley JA, Mwangi T, Ogada E, Mwangi I, Maitland K, Williams T, Scott JAG, English M, Lowe BS, et al. 646 Defining childhood severe falciparum malaria for intervention studies. *PLoS Medicine*. 2007; 4(8):e251.

647 **Carter R**, Mendis KN. Evolutionary and historical aspects of the burden of malaria. *Clinical microbiology reviews*. 648 2002; 15(4):564–594.

649 **Clarke GM**, Rockett K, Kivinen K, Hubbart C, Jeffreys AE, Rowlands K, Jallow M, Conway DJ, Bojang KA, Pinder M, 650 et al. Characterisation of the opposing effects of G6PD deficiency on cerebral malaria and severe malarial 651 anaemia. *eLife*. 2017; 6:e15085.

652 **Dondorp AM**, Fanello CI, Hendriksen IC, Gomes E, Seni A, Chhaganlal KD, Bojang K, Olaosebikan R, Anunobi N, 653 Maitland K, et al. Artesunate versus quinine in the treatment of severe falciparum malaria in African children 654 (AQUAMAT): an open-label, randomised trial. *The Lancet*. 2010; 376(9753):1647–1657.

655 **Dondorp AM**, Nosten F, Stepniewska K, Day N, White N. Artesunate versus quinine for treatment of severe 656 falciparum malaria: a randomised trial. *The Lancet*. 2005; 366(9487):717–725.

657 **Frühwirth-Schnatter S**, Malsiner-Walli G. From here to infinity: sparse finite versus Dirichlet process mixtures 658 in model-based clustering. *Advances in Data Analysis and Classification*. 2019 Mar; 13(1):33–64. <https://doi.org/10.1007/s11634-018-0329-y>, doi: 10.1007/s11634-018-0329-y.

660 **Gérardin P**, Rogier C, Amadou SK, Jouvencel P, Brousse V, Imbert P. Prognostic value of thrombocytopenia 661 in African children with falciparum malaria. *The American Journal of Tropical Medicine and Hygiene*. 2002; 662 66(6):686–691.

663 **Gérardin P**, Rogier C, Amadou SK, Jouvencel P, Diatta B, Imbert P. Outcome of life-threatening malaria in African 664 children requiring endotracheal intubation. *Malaria Journal*. 2007; 6(1):51.

665 **Gomes M**, Faiz M, Gyapong J, Warsame M, Agbenyega T, Babiker A, Baiden F, Yunus E, Binka F, Clerk C, Folb P, Hassan R, Hossain M, Kimbute O, Kitua A, Krishna S, Makasi C, Mensah N, Mrango Z, Olliaro P, et al. Pre-referral rectal artesunate to prevent death and disability in severe malaria: a placebo-controlled trial. *The Lancet*. 2009; 373(9663):557–566. <https://www.sciencedirect.com/science/article/pii/S0140673608617341>, doi: [https://doi.org/10.1016/S0140-6736\(08\)61734-1](https://doi.org/10.1016/S0140-6736(08)61734-1).

670 **Hanson J**, Phu NH, Hasan MU, Charunwatthana P, Plewes K, Maude RJ, Prapansilp P, Kingston HW, Mishra SK, 671 Mohanty S, et al. The clinical implications of thrombocytopenia in adults with severe falciparum malaria: a 672 retrospective analysis. *BMC medicine*. 2015; 13(1):1–9.

673 **Hendriksen IC**, Mwanga-Amumpaire J, Von Seidlein L, Mtove G, White LJ, Olaosebikan R, Lee SJ, Tshefu AK, 674 Woodrow C, Amos B, et al. Diagnosing severe falciparum malaria in parasitaemic African children: a prospective 675 evaluation of plasma PfHRP2 measurement. *PLoS Medicine*. 2012; 9(8):e1001297.

676 **Hien TT**, Day NP, Phu NH, Mai NTH, Chau TTH, Loc PP, Sinh DX, Chuong LV, Vinh H, Waller D, et al. A controlled 677 trial of artemether or quinine in Vietnamese adults with severe falciparum malaria. *New England Journal of 678 Medicine*. 1996; 335(2):76–83.

679 **Kariuki SN**, Williams TN. Human genetics and malaria resistance. *Human Genetics*. 2020; 139(6):801–811. 680 <https://doi.org/10.1007/s00439-020-02142-6>, doi: 10.1007/s00439-020-02142-6.

681 Lanneaux J, Dauger S, Pham LL, Naudin J, Faye A, Gillet Y, Bosdure E, Carbajal R, Dubos F, Vialet R, et al. Retrospective study of imported falciparum malaria in French paediatric intensive care units. *Archives of Disease in Childhood*. 2016; 101(11):1004–1009.

684 Leblanc C, Vasse C, Minodier P, Mornand P, Naudin J, Quinet B, Siriez J, Sorge F, de Suremain N, Thellier M, et al. Management and prevention of imported malaria in children. Update of the French guidelines. *Medecine et maladies infectieuses*. 2020; 50(2):127–140.

687 Leffler EM, Band G, Busby GB, Kivinen K, Le QS, Clarke GM, Bojang KA, Conway DJ, Jallow M, Sisay-Joof F, et al. Resistance to malaria through structural variation of red blood cell invasion receptors. *Science*. 2017; 356(6343).

689 Leopold SJ, Watson JA, Jeeyapant A, Simpson JA, Phu NH, Hien TT, Day NP, Dondorp AM, White NJ. Investigating causal pathways in severe falciparum malaria: A pooled retrospective analysis of clinical studies. *PLoS Medicine*. 2019; 16(8).

692 Maitland K, Kiguli S, Opoka RO, Engoru C, Oliupot-Oliupot P, Akech SO, Nyeko R, Mtove G, Reyburn H, Lang T, et al. Mortality after fluid bolus in African children with severe infection. *New England Journal of Medicine*. 2011; 364(26):2483–2495.

695 Mornand P, Verret C, Minodier P, Faye A, Thellier M, Imbert P, for the 'Centre National de Référence du Paludisme' PIMSG. Severe imported malaria in children in France. A national retrospective study from 1996 to 2005. *PLoS ONE*. 2017; 12(7):e0180758.

698 Ndila CM, Uyoga S, Macharia AW, Nyutu G, Peshu N, Ojal J, Shebe M, Awuondo KO, Mturi N, Tsofa B, et al. Human candidate gene polymorphisms and risk of severe malaria in children in Kilifi, Kenya: a case-control association study. *The Lancet Haematology*. 2018; 5(8):e333–e345.

701 Ndila C, Nyirongo V, Macharia A, Jeffreys A, Rowlands K, Hubbard C, Busby G, Band G, Harding R, Rockett K, Williams T, null n. Haplotype heterogeneity and low linkage disequilibrium reduce reliable prediction of genotypes for the $\alpha^{3.71}$ form of α -thalassaemia using genome-wide microarray data [version 1; peer review: awaiting peer review]. *Wellcome Open Research*. 2020; 5(287). doi: [10.12688/wellcomeopenres.16320.1](https://doi.org/10.12688/wellcomeopenres.16320.1).

705 Nie L, Zhang Z, Rubin D, Chu J, et al. Likelihood reweighting methods to reduce potential bias in noninferiority trials which rely on historical data to make inference. *The Annals of Applied Statistics*. 2013; 7(3):1796–1813.

707 Opi DH, Ochola LB, Tendwa M, Siddondo BR, Ocholla H, Fanjo H, Ghumra A, Ferguson NJ, Rowe JA, Williams TN. Mechanistic studies of the negative epistatic malaria-protective interaction between sickle cell trait and $\alpha+$ thalassemia. *EBioMedicine*. 2014; 1(1):29–36.

710 Phu NH, Tuan PQ, Day N, Mai NT, Chau TT, Chuong LV, Sinh DX, White NJ, Farrar J, Hien TT. Randomized controlled trial of artesunate or artemether in Vietnamese adults with severe falciparum malaria. *Malaria Journal*. 2010; 9(1):97.

713 Phu NH, Day NPJ, Tuan PQ, Mai NTH, Chau TTH, Van Chuong L, Vinh H, Loc PP, Sinh DX, Hoa NTT, Waller DJ, Wain J, Jeeyapant A, Watson JA, Farrar JJ, Hien TT, Parry CM, White NJ. Concomitant Bacteremia in Adults With Severe Falciparum Malaria. *Clinical Infectious Diseases*. 2020 02; <https://doi.org/10.1093/cid/ciaa191>, doi: 10.1093/cid/ciaa191, ciaa191.

717 Reich D, Nalls MA, Kao WL, Akylbekova EL, Tandon A, Patterson N, Mullikin J, Hsueh WC, Cheng CY, Coresh J, et al. Reduced neutrophil count in people of African descent is due to a regulatory variant in the Duffy antigen receptor for chemokines gene. *PLoS Genetics*. 2009; 5(1):e1000360.

720 Rodriguez-Barraquer I, Arinaitwe E, Jagannathan P, Kamya MR, Rosenthal PJ, Rek J, Dorsey G, Nankabirwa J, Staedke SG, Kilama M, et al. Quantification of anti-parasite and anti-disease immunity to malaria as a function of age and exposure. *eLife*. 2018; 7:e35832.

723 Sadarangani M, Makani J, Komba AN, Ajala-Agbo T, Newton CR, Marsh K, Williams TN. An observational study of children with sickle cell disease in Kilifi, Kenya. *British Journal of Haematology*. 2009; 146(6):675–682.

725 Scott JAG, Berkley JA, Mwangi I, Ochola L, Uyoga S, MacHaria A, Ndila C, Lowe BS, Mwarumba S, Bauni E, Marsh K, Williams TN. Relation between falciparum malaria and bacteraemia in Kenyan children: A population-based, case-control study and a longitudinal study. *The Lancet*. 2011; 378(9799):1316–1323. [http://dx.doi.org/10.1016/S0140-6736\(11\)60888-X](http://dx.doi.org/10.1016/S0140-6736(11)60888-X), doi: 10.1016/S0140-6736(11)60888-X.

729 Small DS, Taylor TE, Postels DG, Beare NA, Cheng J, MacCormick IJ, Seydel KB. Evidence from a natural experiment that malaria parasitemia is pathogenic in retinopathy-negative cerebral malaria. *eLife*. 2017; 6:e23699.

731 **Smith T**, Schellenberg JA, Hayes R. Attributable fraction estimates and case definitions for malaria in endemic.
732 Statistics in Medicine. 1994; 13(22):2345–2358.

733 **Stan Development Team**, RStan: the R interface to Stan; 2020. <http://mc-stan.org/>, r package version 2.21.2.

734 **Storey JD**. A direct approach to false discovery rates. Journal of the Royal Statistical Society: Series B (Statistical
735 Methodology). 2002; 64(3):479–498.

736 **Taylor SM**, Parobek CM, Fairhurst RM. Haemoglobinopathies and the clinical epidemiology of malaria: a sys-
737 tematic review and meta-analysis. The Lancet Infectious Diseases. 2012; 12(6):457–468.

738 **Taylor TE**, Fu WJ, Carr RA, Whitten RO, Mueller JG, Fosiko NG, Lewallen S, Liomba NG, Molyneux ME. Differenti-
739 ating the pathologies of cerebral malaria by postmortem parasite counts. Nature Medicine. 2004; 10(2):143–
740 145.

741 **Teo YY**, Small KS, Kwiatkowski DP. Methodological challenges of genome-wide association analysis in Africa.
742 Nature Reviews Genetics. 2010; 11(2):149–160.

743 **The Malaria Genomic Epidemiology Network**. Reappraisal of known malaria resistance loci in a large multi-
744 center study. Nature Genetics. 2014; 46(11):1197.

745 **Uyoga S**, Macharia AW, Ndila CM, Nyutu G, Shebe M, Awuondo KO, Mturi N, Peshu N, Tsofa B, Scott JAG, Maitland
746 K, Williams TN. The indirect health effects of malaria estimated from health advantages of the sickle cell trait.
747 Nature Communications. 2019; 10(1):856. <https://doi.org/10.1038/s41467-019-08775-0>, doi: 10.1038/s41467-019-08775-0.

749 **Uyoga S**, Ndila CM, Macharia AW, Nyutu G, Shah S, Peshu N, Clarke GM, Kwiatkowski DP, Rockett KA, Williams
750 TN, et al. Glucose-6-phosphate dehydrogenase deficiency and the risk of malaria and other diseases in
751 children in Kenya: a case-control and a cohort study. The Lancet Haematology. 2015; 2(10):e437–e444.

752 **Wambua S**, Mwangi TW, Kortok M, Uyoga SM, Macharia AW, Mwacharo JK, Weatherall DJ, Snow RW, Marsh K,
753 Williams TN. The effect of α^+ -thalassaemia on the incidence of malaria and other diseases in children living
754 on the coast of Kenya. PLoS Medicine. 2006; 3(5):e158.

755 **Warrell DA**, Looareesuwan S, Warrell MJ, Kasemsarn P, Intaraprasert R, Bunnag D, Harinasuta T. Dexam-
756 ethasone Proves Deleterious in Cerebral Malaria. New England Journal of Medicine. 1982; 306(6):313–319.
757 <https://doi.org/10.1056/NEJM198202113060601>, doi: 10.1056/NEJM198202113060601, PMID: 7033788.

758 **Watson JA**, Leopold SJ, Simpson JA, Day NP, Dondorp AM, White NJ. Collider bias and the apparent protective
759 effect of glucose-6-phosphate dehydrogenase deficiency on cerebral malaria. eLife. 2019; 8:e43154.

760 **White NJ**, Turner GD, Day NP, Dondorp AM. Lethal malaria: Marchiafava and Bignami were right. The Journal
761 of Infectious Diseases. 2013; 208(2):192–198.

762 **Williams TN**, Mwangi TW, Wambua S, Peto TE, Weatherall DJ, Gupta S, Recker M, Penman BS, Uyoga S, Macharia
763 A, et al. Negative epistasis between the malaria-protective effects of α^+ -thalassemia and the sickle cell trait.
764 Nature Genetics. 2005; 37(11):1253–1257.

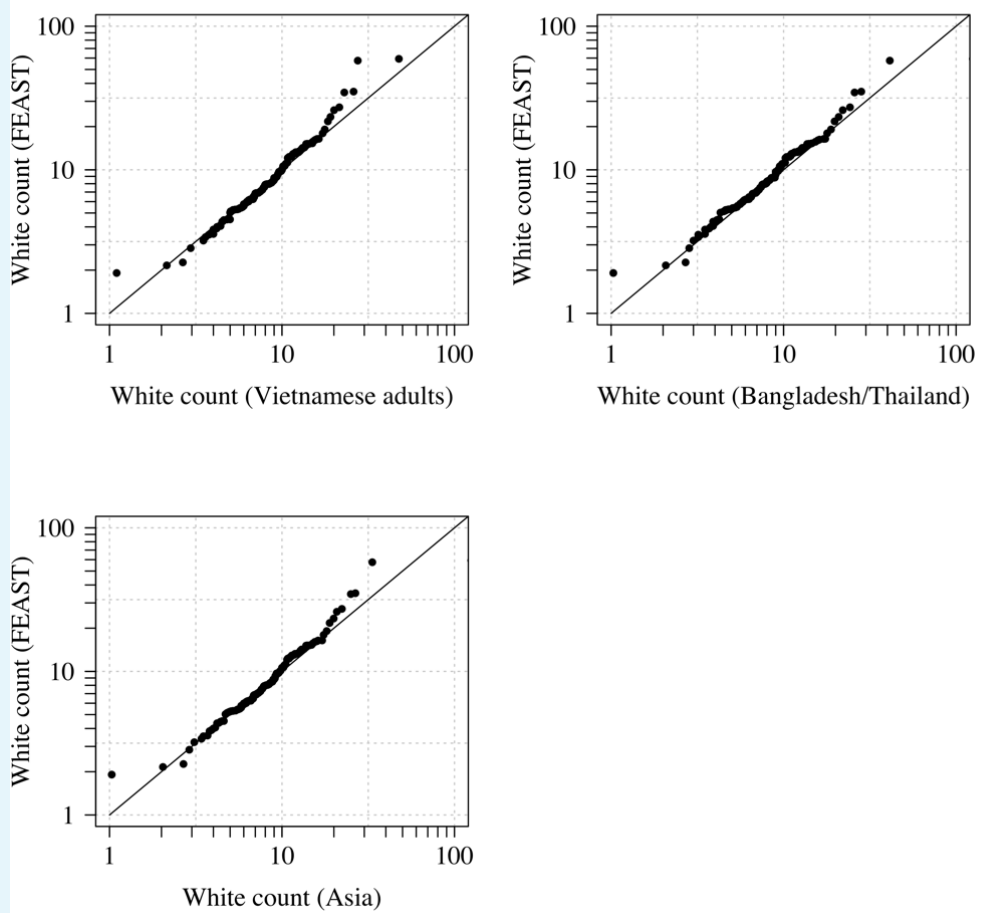
765 **Williams TN**, Obaro SK. Sickle cell disease and malaria morbidity: a tale with two tails. Trends in parasitology.
766 2011; 27(7):315–320.

767 **World Health Organisation**. Severe Malaria. Tropical Medicine & International Health. 2014; 19(Supplement
768 1):7–131. https://onlinelibrary.wiley.com/doi/abs/10.1111/tmi.12313_2, doi: 10.1111/tmi.12313_2.

769 **World Health Organization**. World malaria report 2020: 20 years of global progress and challenges; 2020.

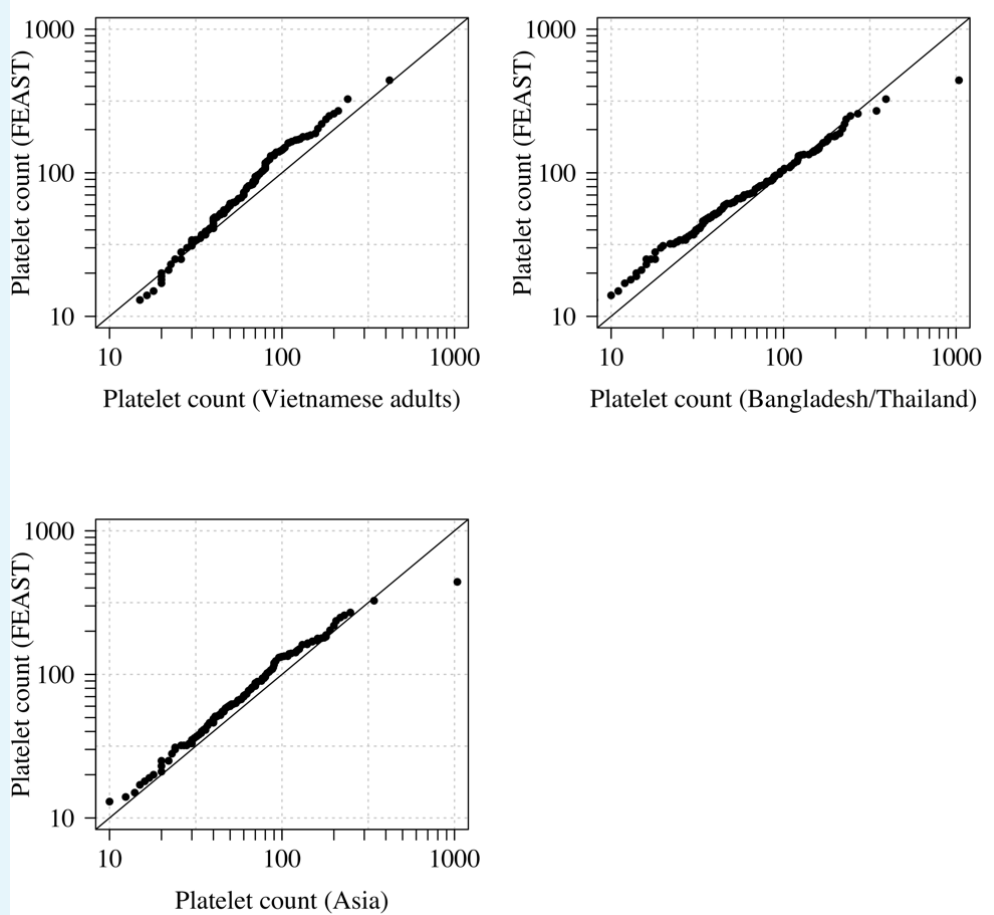
770 **Zondervan KT**, Cardon LR. Designing candidate gene and genome-wide case-control association studies. Na-
771 ture Protocols. 2007; 2(10):2492–2501. <https://doi.org/10.1038/nprot.2007.366>, doi: 10.1038/nprot.2007.366.

772 **Appendix 1**



773
774
775
776
777
778
779

Appendix 1 Figure 1. Comparison of the marginal distributions of white blood cell counts between Asian adults and children with severe malaria and African children with severe malaria. FEAST: 121 severely ill Ugandan children with $PfHRP2 > 1,000 \text{ ng/mL}$ (Maitland et al., 2011). Vietnamese adults: 930 adults from two large randomised trials in severe malaria (Phu et al., 2010; Hien et al., 1996). Bangladesh/Thailand: 653 adults and children from observational studies of severe malaria (Leopold et al., 2019).

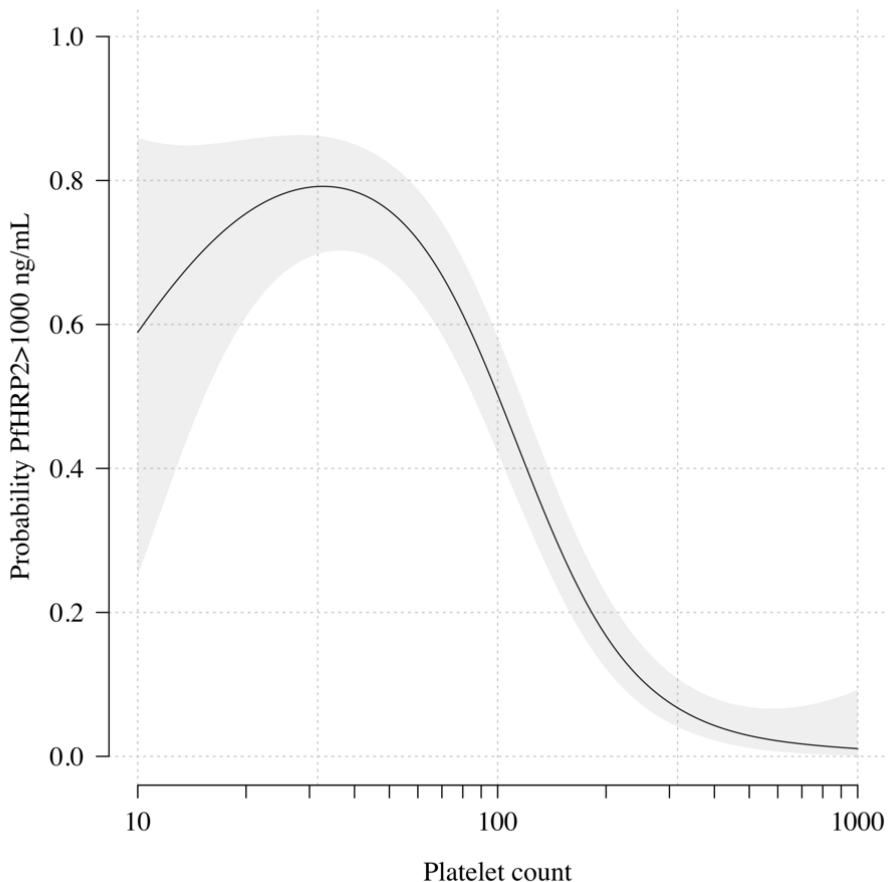


781
782
783
784
785
786
787
788
789

Appendix 1 Figure 2. Comparison of the marginal distributions of platelet counts between Asian adults and children with severe malaria and African children with severe malaria. FEAST: 121 severely ill Ugandan children with *Pf*HRP2 > 1,000 ng/mL (Maitland *et al.*, 2011). Vietnamese adults: 930 adults from two large randomised trials in severe malaria (Phu *et al.*, 2010; Hien *et al.*, 1996). Bangladesh/Thailand: 653 adults and children from observational studies of severe malaria (Leopold *et al.*, 2019). The bottom left qqplot compares the white counts from the children in the FEAST study with the combined dataset from Vietnam and Bangladesh/Thailand.

790 **Appendix 2**

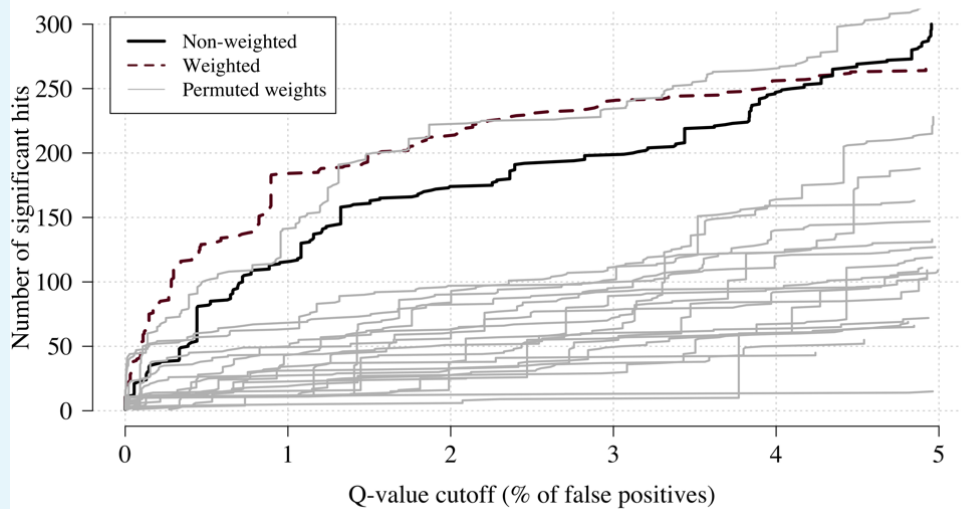
Severely ill African children (FEAST)



791
792
793
794
795
796
797
798
800

Appendix 2 Figure 1. The relationship between platelet counts and plasma PfHRP2 in severely ill African children. The black line (shaded area) shows the estimated probability (95% confidence interval) that the plasma PfHRP2 > 1,000 ng/mL as a function of \log_{10} platelet count. This fit is derived from a generalised additive logistic regression model ($p < 10^{-16}$ for the spline term), fit using the R package *mgcv*. The generalised additive model was fit to data from 566 African children enrolled in the FEAST trial (Maitland *et al.*, 2011) (all the children who had both platelet counts and PfHRP2 data available). Plasma PfHRP2 > 1,000 ng/mL is highly discriminatory for severe malaria (Hendriksen *et al.*, 2012).

801 **Appendix 3**

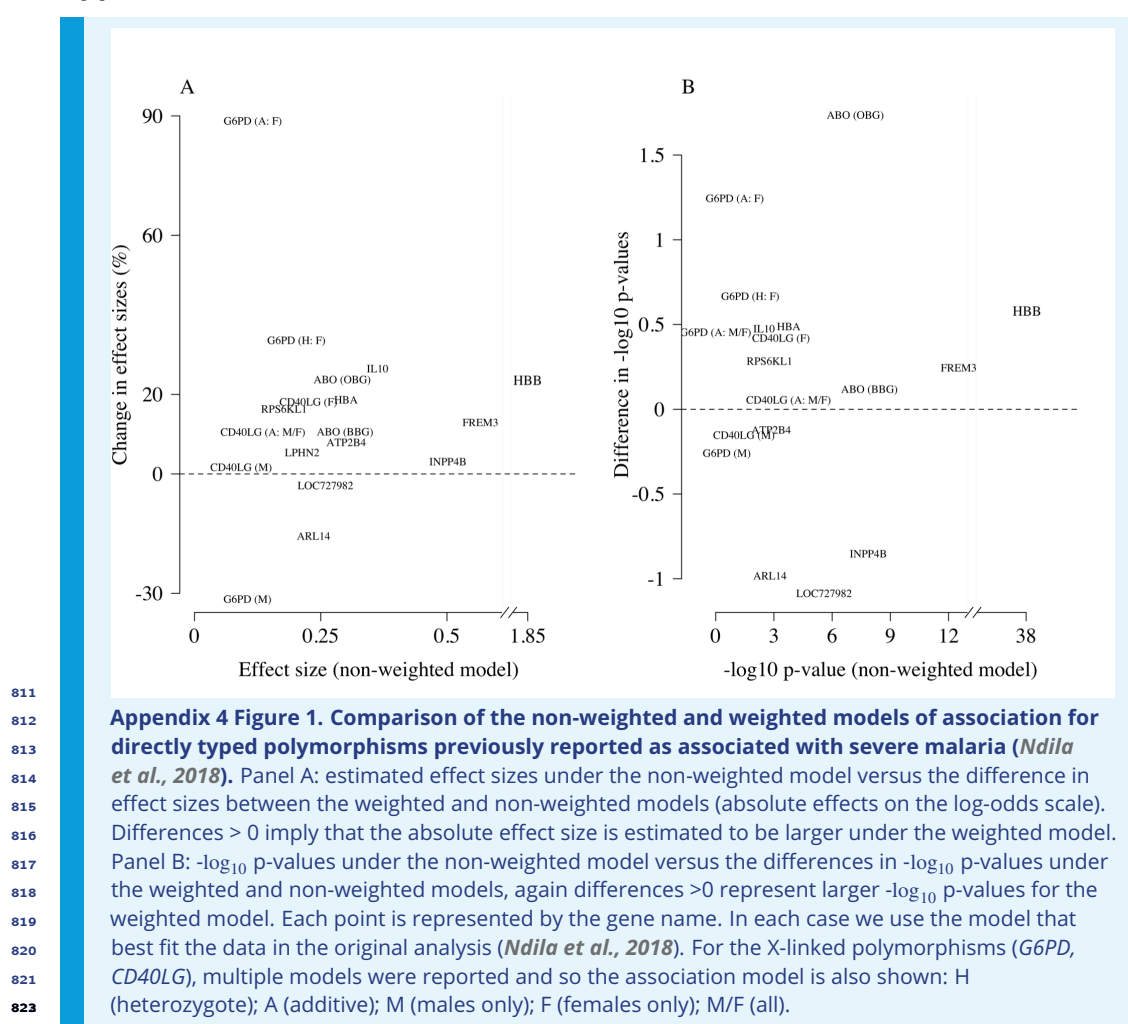


802
803
804
805
806
807
808

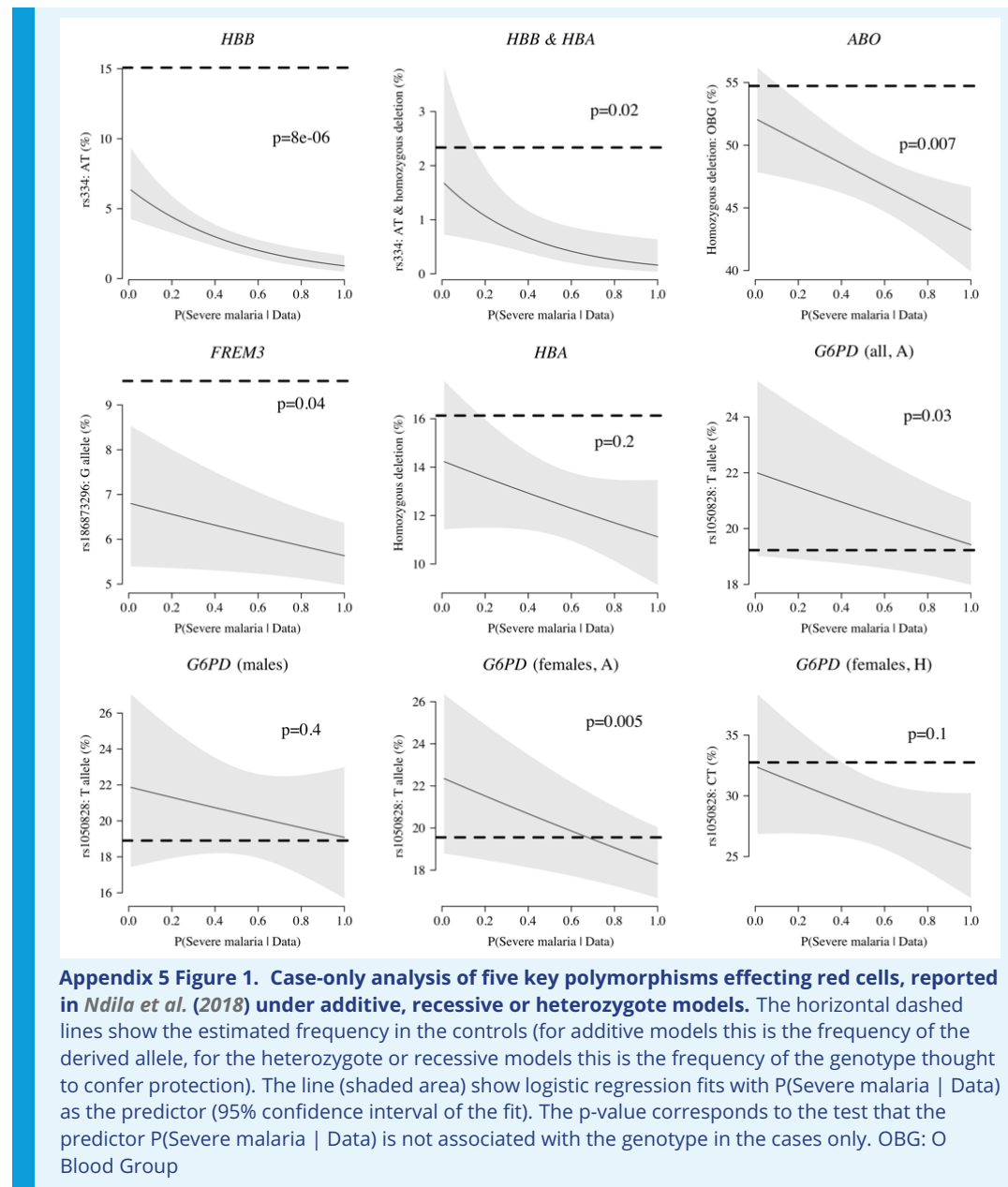
Appendix 3 Figure 1. Effect of permuting the weights in the re-weighted (data-tilting) GWAS.

Here we show the results of 20 random permutations of the weights, applied to the Kenyan case-control GWAS using only chromosomes 4, 9 and 11 (where the top hits are - we limit it to these 3 chromosomes for computational reasons). The random permutations (grey) decrease the number of significant hits compared to the non-weighted (thick black) and the non-permuted re-weighted model (dashed purple).

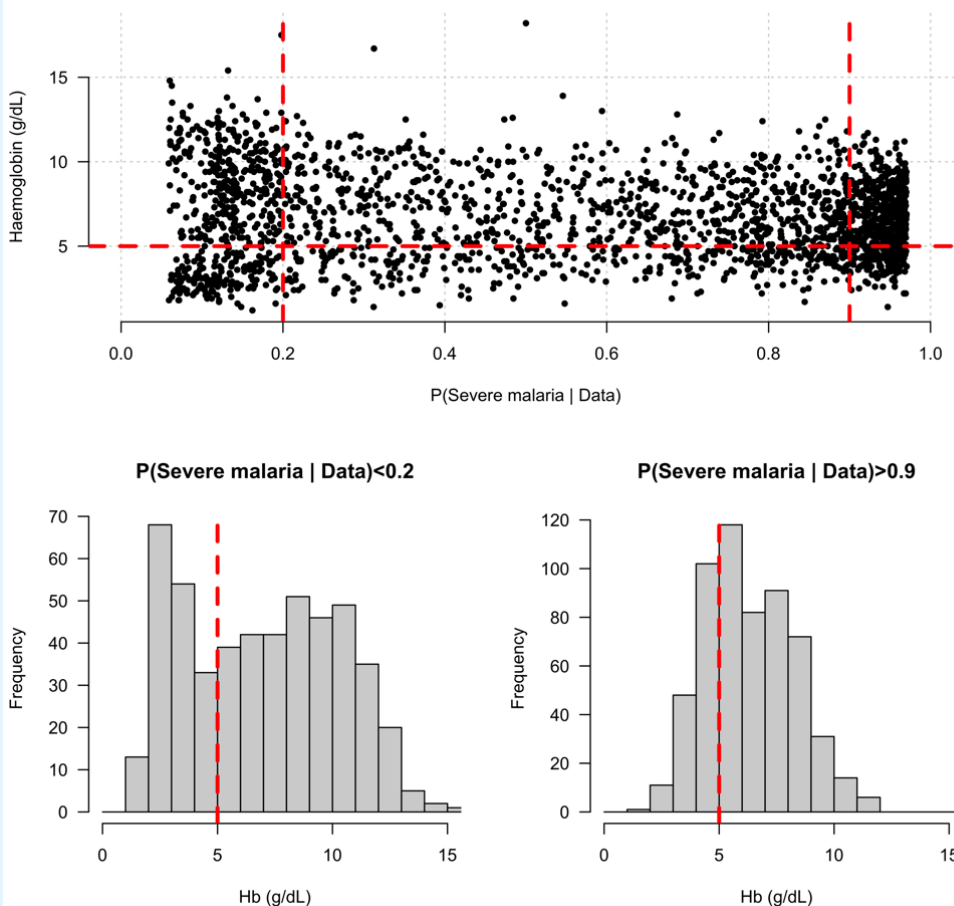
810 **Appendix 4**



824 **Appendix 5**

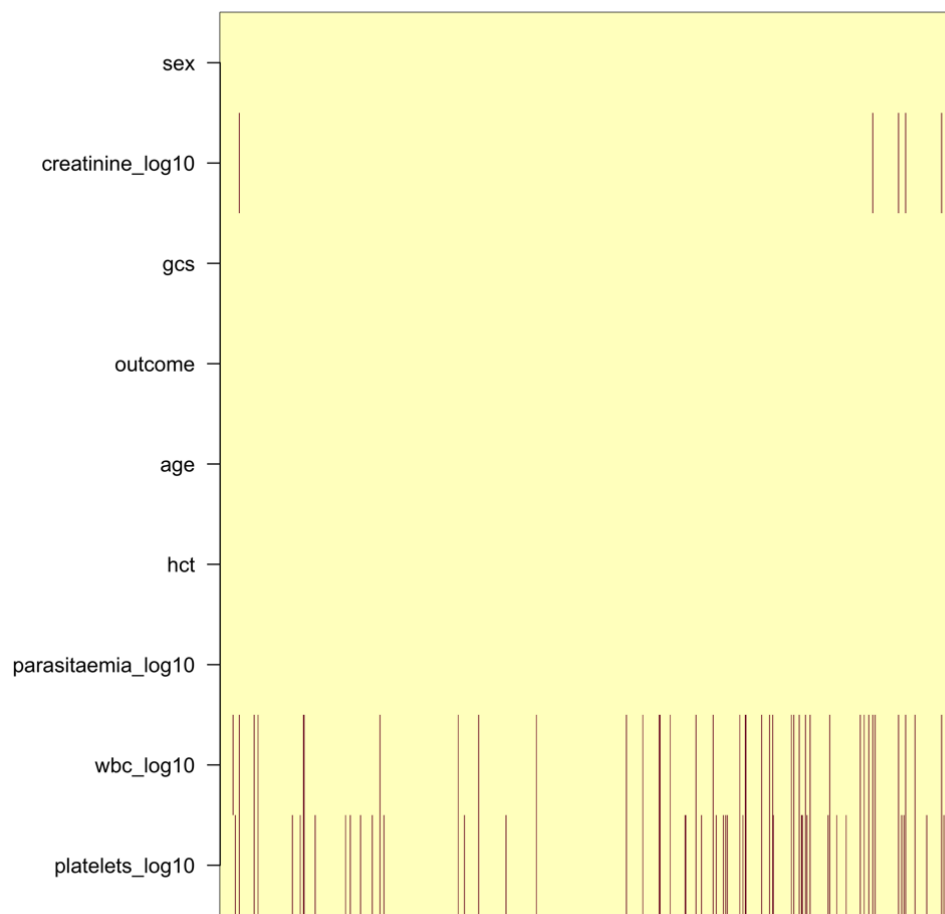


835 **Appendix 6**



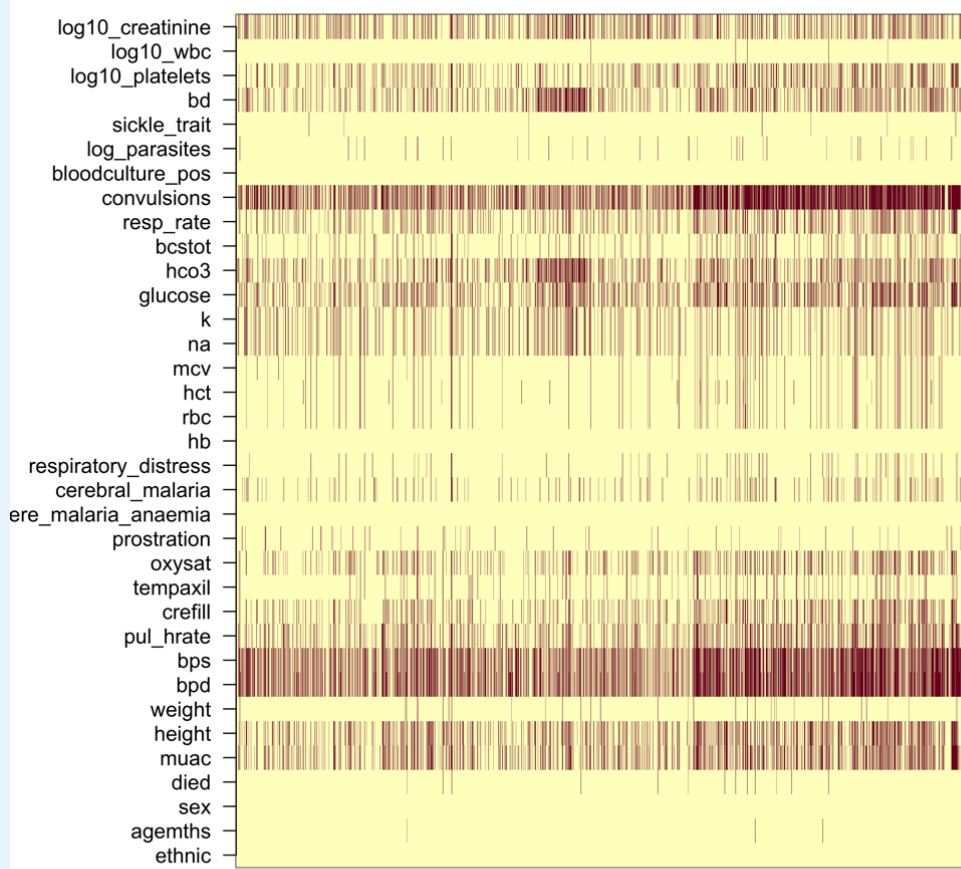
Appendix 6 Figure 1. Distribution of admission haemoglobin concentrations as a function of $P(\text{Severe malaria} | \text{Data})$. Severe anaemia is generally defined as a haemoglobin less than 5 g/dL in African children diagnosed with severe malaria, shown by the horizontal dashed red line in the top panel and the vertical dashed red lines in the bottom panels. The vertical dashed red lines in the top panel show the top and bottom quintiles of the probability distribution (0.9 and 0.2, respectively). Patients in the bottom quintile of the probability distribution had a markedly bi-modal distribution in haemoglobin concentrations with a substantial proportion meeting the severe anaemia criterion and a substantial proportion with relatively high haemoglobin concentrations (> 10 g/dL), suggesting two patients subgroups. Patients in the top quintile had a uni-modal distribution of haemoglobin.

847 **Appendix 7**



848
849
850
852

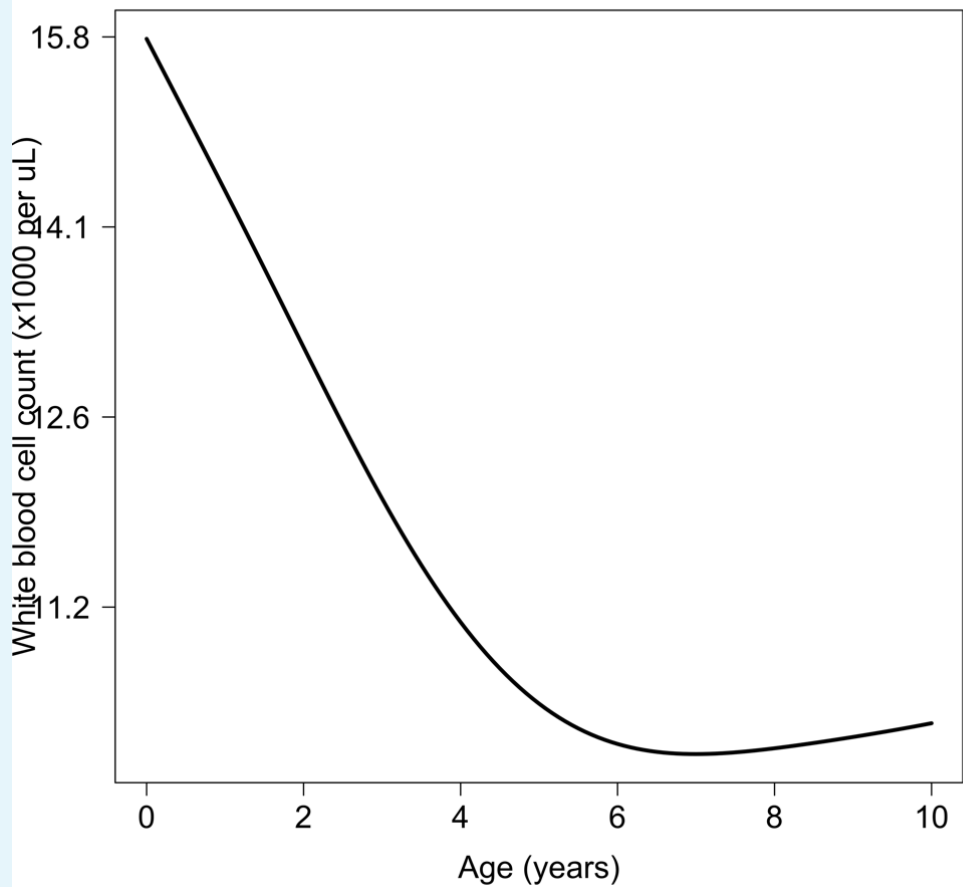
Appendix 7 Figure 1. Pattern of missing clinical data in the 930 Vietnamese adults. These data pool the AQ Vietnam severe malaria study (*Hien et al., 1996*) and the AAV severe malaria study (*Phu et al., 2010*) (red: missing; yellow: recorded).



853
854
855

Appendix 7 Figure 2. Missing clinical data in the 2,220 Kenyan children diagnosed with severe malaria . (red: missing; yellow: recorded).

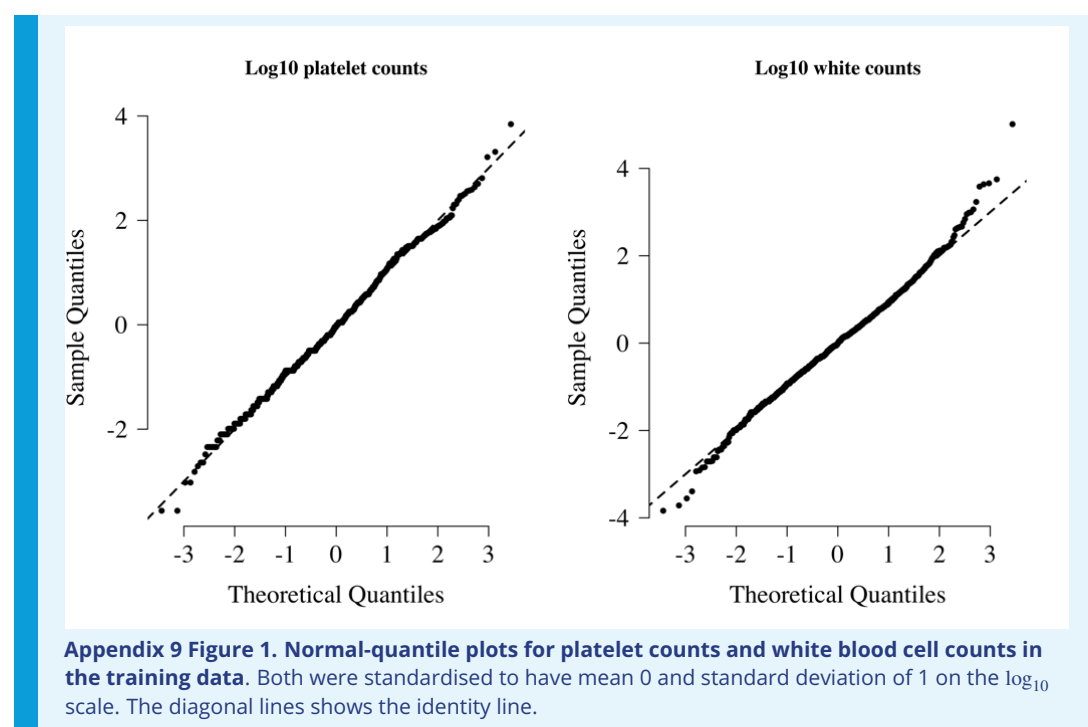
857 **Appendix 8**



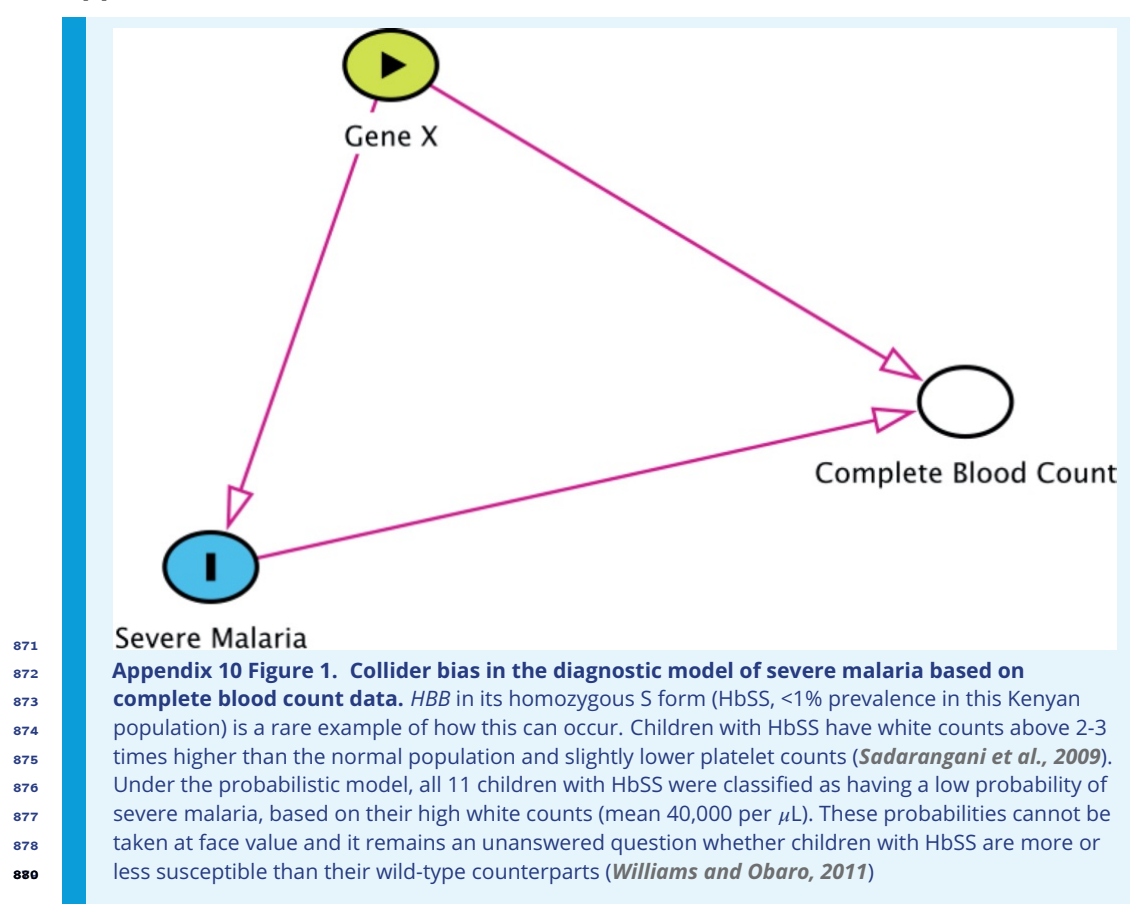
858
859
860
861
863

Appendix 8 Figure 1. Relationship between age and mean white count (modelled on the \log_{10} scale). This is estimated from 858 children in the FEAST trial who had white counts available using a additive linear model ($p = 10^{-8}$ for the smooth spline term). We used this model to adjust observed \log_{10} white counts in all children less than 5 years of age in the training and testing datasets.

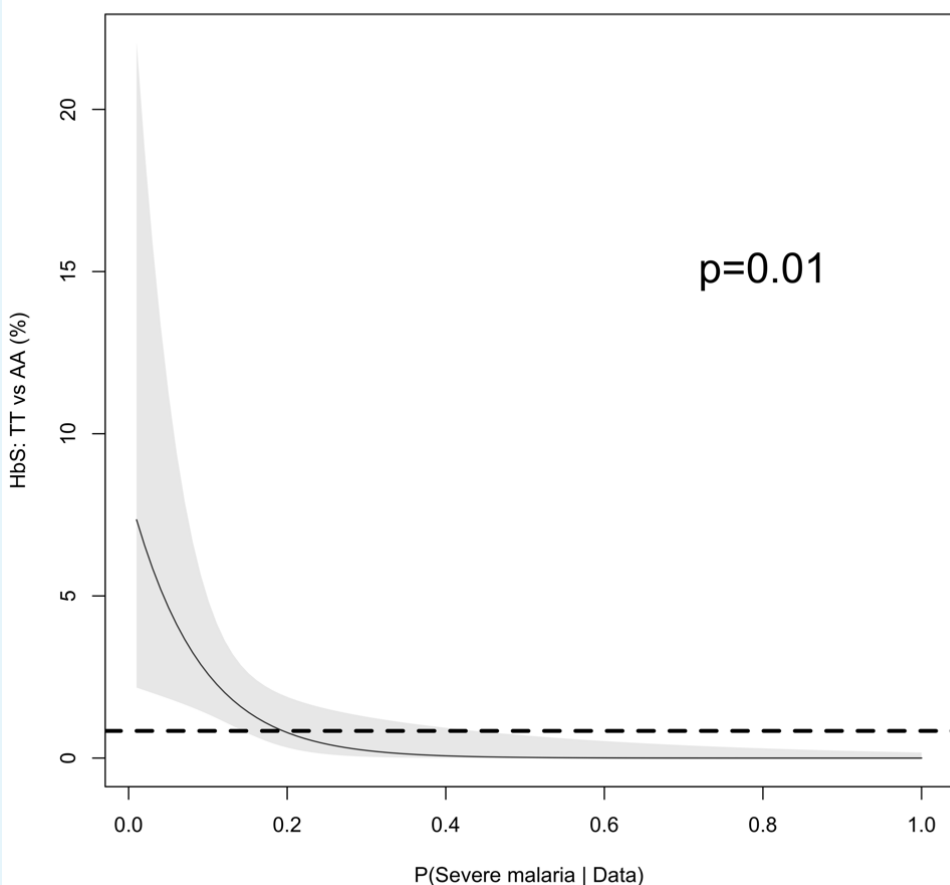
864 **Appendix 9**



870 Appendix 10



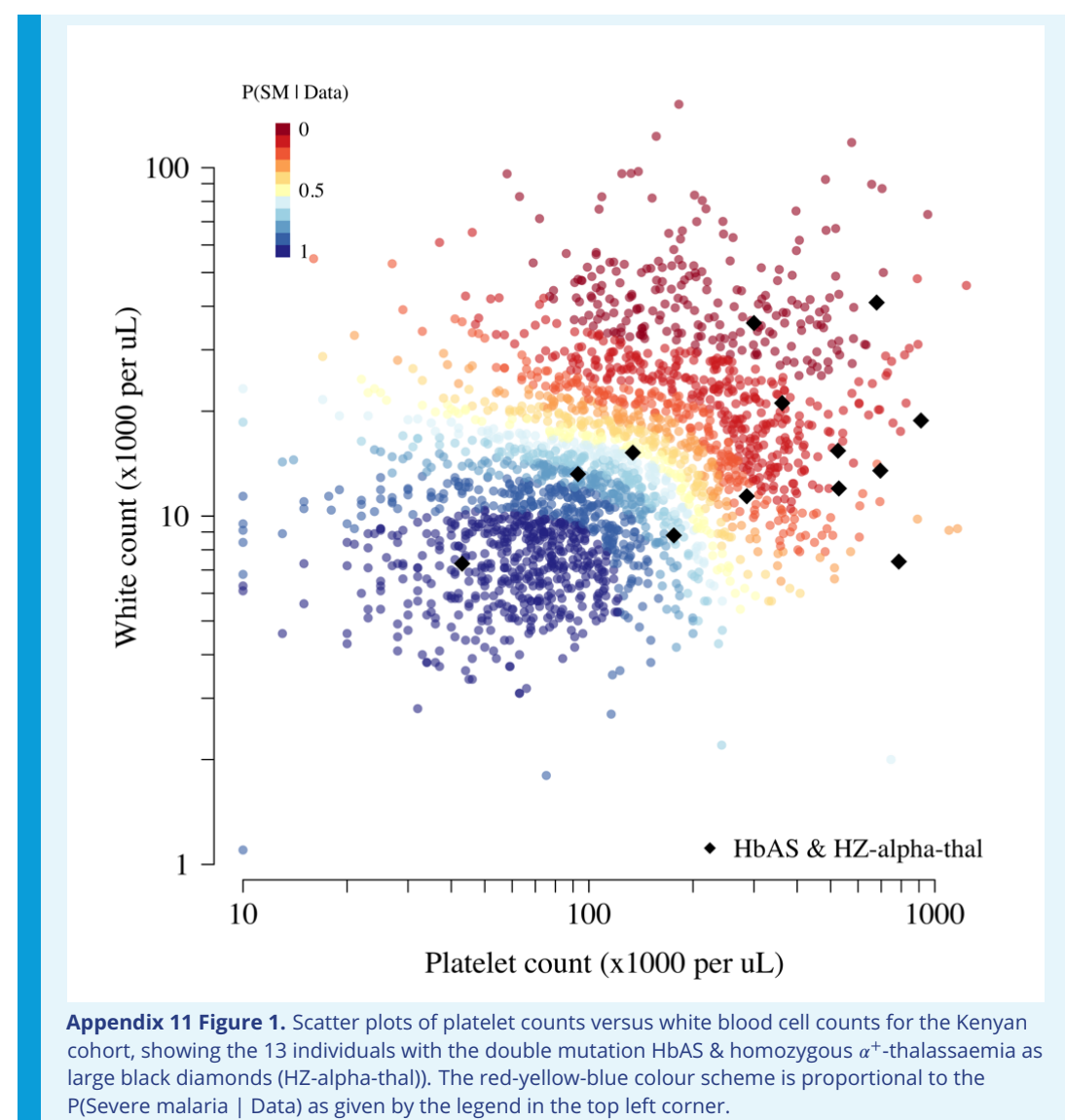
Sickle cell anaemia



881
882
883
884
885
886
887

Appendix 10 Figure 2. The relationship between HbSS and the estimated probabilities of severe malaria under the diagnostic model. There were 11 children with HbSS and they all had low probabilities of severe malaria but this is biased as these children have chronic inflammation with white counts 2-3 higher than the general population (*Sadarangani et al., 2009*) (see above Figure for the causal diagram showing collider bias).

888 **Appendix 11**



895 Appendix 12

896 Simulation study

897 To demonstrate how the re-weighted likelihood works on simulated data where the true
898 latent classes are known, we constructed the following simulation assuming:

899

900

901

902

903

904

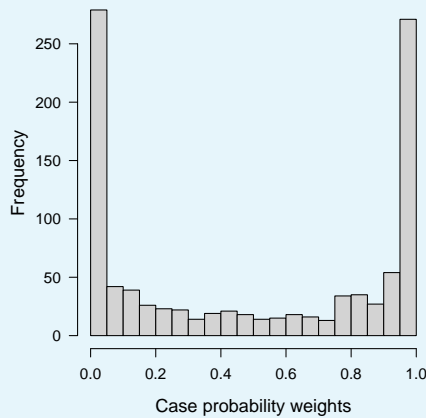
905

906

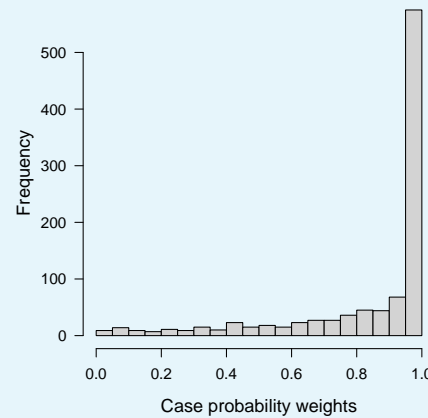
- A biallelic marker with a derived allele frequency of 10% in the control population (diplotypes encoded as 0, 1, 2).
- An additive protective effect for the true cases resulting in a derived allele frequency of 7% in the true cases; no effect in the false cases.
- The latent class probability weights for the true cases are drawn from a Beta(0.2, 1) distribution, and the probability weights for the false cases are drawn from a Beta(1, 0.2) distribution.
- A proportion of true versus false cases varying between 50 and 100%.

907 The R code for the simulation is given in the file `Simulation_study_weightedLikelihood.R`
908 in the github repository https://github.com/jwatowatson/Kenyan_phenotypic_accuracy. Figures
909 1 and 2 show how the estimates effect sizes, the standard errors and the power (1-type 2
910 error) vary as a function of the proportion of the true cases.

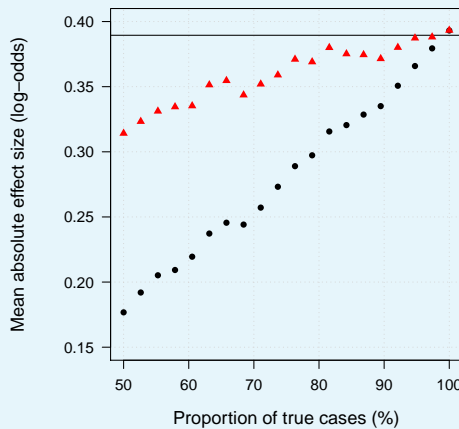
A



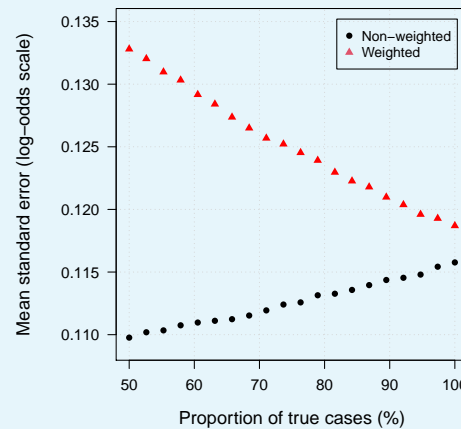
B



C



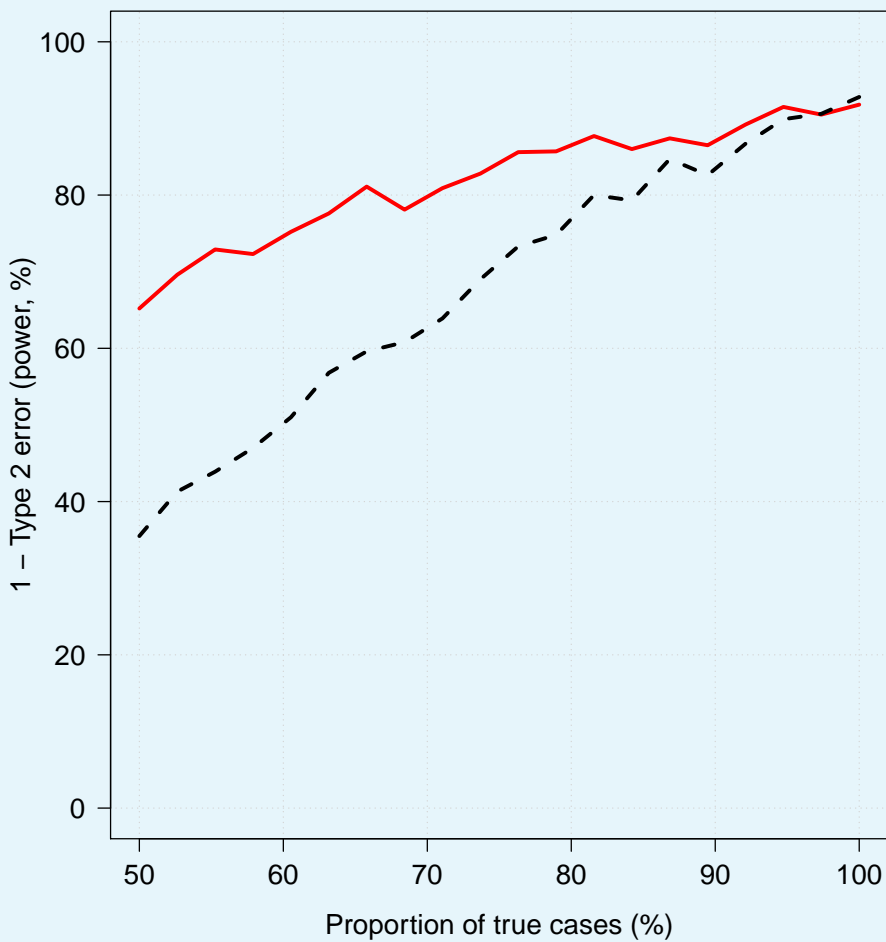
D



911

912
913
914
915
916
917
918

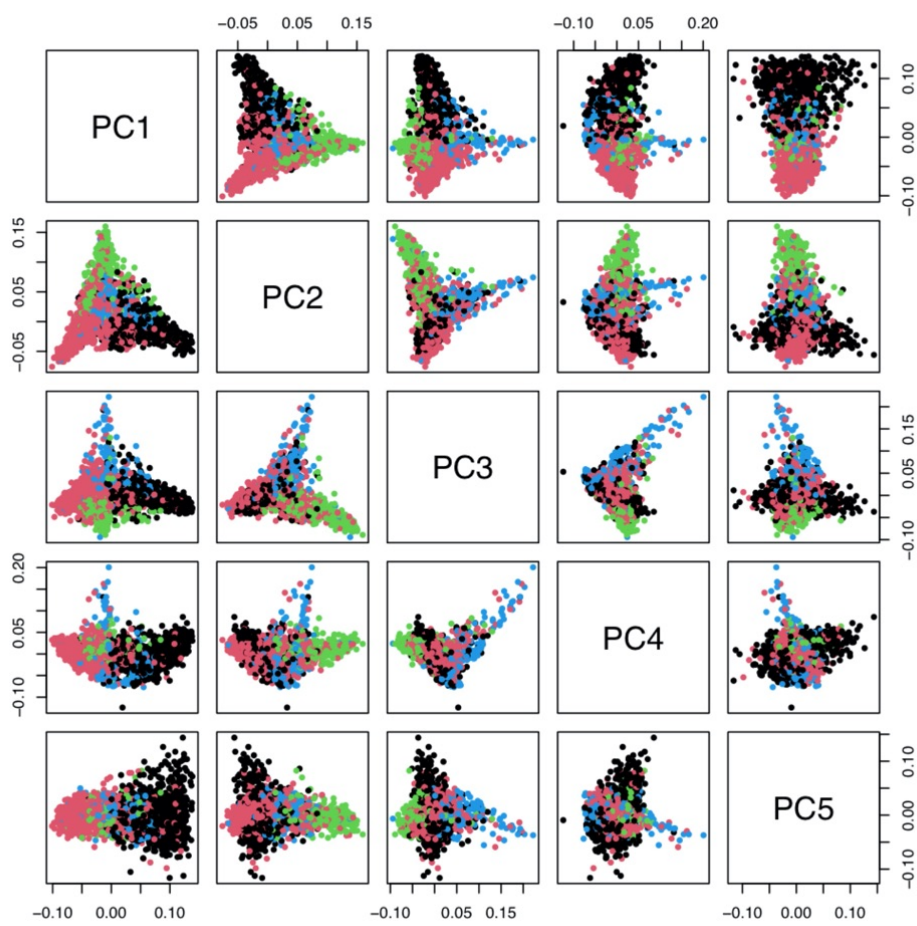
Appendix 12 Figure 1. Simulation study demonstrating how likelihood re-weighting can improve estimation accuracy in case-control studies. Panels A and B show histograms of the case probability weights used in the simulations for the scenarios when 50% of cases are true cases, and when 100% of cases are true cases, respectively. Panel C: estimated effect sizes as a function of the proportion of mis-classified cases. Panel D: standard errors of effect estimates as a proportion of mis-classified cases.



919
920
921
922

Appendix 12 Figure 2. Effect of case re-weighting on power (1-type 2 error). The thick red line shows the estimated power for the re-weighted approach; the dashed black line shows the estimated power for the non-weighted approach.

924 **Appendix 13**



925
926
927
928
930

Appendix 13 Figure 1. Principal components analysis of 1,666 Kenyan cases and 1,606 population controls. The colours show the main self-reported ethnicities (black: Chonyi; red: Girima; green: Kauma; blue: other). The first 5 principal components were used to stratify for population structure in the GWAS analyses.